Kaunas University of Technology
Faculty of Mathematics and Natural Sciences

Development of an Open Source Gamma Spectrometer

Master's Final Degree Project

Justas Beresnevičius
Project author

assoc. prof. dr. Benas Gabrielis Urbonavičius
Supervisor

Kaunas, 2022

Kaunas University of Technology
Faculty of Mathematics and Natural Sciences

Development of an Open Source Gamma Spectrometer

Master's Final Degree Project
Medical Physics (6213GX001)

Justas Beresnevičius
Project author

assoc. prof. dr. Benas Gabrielis Urbonavičius
Supervisor

Mantvydas Merkis
Reviewer

Kaunas, 2022

Kaunas University of Technology

Faculty of Mathematics and Natural Sciences

Justas Beresnevičius

Development of an Open Source Gamma Spectrometer

Declaration of Academic Integrity

I confirm the following:

1. I have prepared the final degree project independently and honestly without any violations of the copyrights or other rights of others, following the provisions of the Law on Copyrights and Related Rights of the Republic of Lithuania, the Regulations on the Management and Transfer of Intellectual Property of Kaunas University of Technology (hereinafter – University) and the ethical requirements stipulated by the Code of Academic Ethics of the University;

2. All the data and research results provided in the final degree project are correct and obtained legally; none of the parts of this project are plagiarised from any printed or electronic sources; all the quotations and references provided in the text of the final degree project are indicated in the list of references;

3. I have not paid anyone any monetary funds for the final degree project or the parts thereof unless required by the law;

4. I understand that in the case of any discovery of the fact of dishonesty or violation of any rights of others, the academic penalties will be imposed on me under the procedure applied at the University; I will be expelled from the University and my final degree project can be submitted to the Office of the Ombudsperson for Academic Ethics and Procedures in the examination of a possible violation of academic ethics.

Justas Beresnevičius

Confirmed electronically

Justas Beresnevičius. Development of an Open Source Gamma Spectrometer. Master's Final Degree Project / assoc. prof. dr. Benas Gabrielis Urbonavičius; Faculty of Mathematics and Natural Sciences, Kaunas University of Technology.

Study field and area (study field group): Medical technologies, Health Sciences.

Keywords: gamma spectrometer; open source; scintillation detector

Kaunas, 2022. 65 p.

Summary

Continuous background measurements and identification of unknown radioactive materials are inherent subjects to the fields of radiation protection and medical physics. Gamma ray spectrometers based on scintillation detector are common devices for such use in border control or nationwide early warning alert systems for radiation hazards due to their ease of use, yet its cost is way above any interested citizen scientist could spend on a hobby.

This work examines a way how to make a reliable gamma spectrometer using scintillating crystal and photomultiplier tube synergy to transmit information about the energy of captured particle. Also, with the help of modern device "GS-USB-PRO" which has a high voltage power supply and analog-to-digital converter inside it is possible to receive the signal from the detector in any device that has an USB or 3.5mm audio jack input.

Using open-source software to analyze the received signal the results showed that developed detector has working voltage of 860V. as well as an energy resolution of ^{137}Cs photopeak of 7.3%, which is 11.6% better than commercially manufactured device "IdentiFINDER". Also, signature energies of ^{137}Cs, ^{133}Ba, ^{228}Th, ^{152}Eu and ^{226}Ra are easily noticeable with constructed device, and proved to let analyze unknown radioactive materials successfully.

Beresnevičius, Justas. Atvirojo kodo gama spektrometro kūrimas. Magistro baigiamasis projektas / doc. dr. Benas Gabrielis Urbonavičius; Kauno technologijos universitetas, Matematikos ir gamtos mokslų fakultetas.

Studijų kryptis ir sritis (studijų krypčių grupė): Medicinos technologijos, Sveikatos mokslai.

Reikšminiai žodžiai: gama spektrometrija, scintiliacinis detektorius.

Kaunas, 2022. 65 p.

Santrauka

Nuolatiniai fono matavimai ir nežinomų radioaktyviųjų medžiagų identifikavimas yra neatskiriami radiacinės saugos ir medicinos fizikos dalykai. Gama spindulių spektrometrai, pagrįsti scintiliacinių detektoriumi, yra įprasti įrenginiai, naudojami pasienio kontrolėje arba visos šalies išankstinio įspėjimo apie radiacijos pavojų sistemose dėl jų naudojimo paprastumo, tačiau jų kaina yra daug didesnė, nei bet kuris suinteresuotas žmogus galėtų išleisti savo pomėgiui.

Šiame darbe nagrinėjamas būdas, kaip sukurti patikimą gama spektrometrą, naudojant scintiliacinių kristalų ir fotodaugiklio vamzdžių sinergiją, siekiant perduoti informaciją apie užfiksuotos dalelės energiją. Taip pat naudojant modernų įrenginį „GS-USB-PRO“, kurio viduje yra aukštos įtampos maitinimo šaltinis ir analoginis-skaitmeninis keitiklis, signalą iš detektoriaus galima priimti bet kuriame įrenginyje, kuris turi USB arba 3,5 mm. garso lizdo įvestis.

Gautam signalui analizuoti naudojant atvirojo kodo programinę įrangą, rezultatai parodė, kad sukurtas detektorius turi 860 V darbinę įtampą. taip pat ^{137}Cs fotosmailės energijos skiriamoji geba yra 7,3%, o tai 11,6% geresnė nei komerciškai prieinamas įrenginys „IdentiFINDER“. Be to, ^{137}Cs, ^{133}Ba, ^{228}Th, ^{152}Eu ir ^{226}Ra energijos yra lengvai pastebimos gautame spektre iš sukonstruoto įrenginio ir įrodė, kad įmanomą sėkmingai analizuoti nežinomas radioaktyviąsias medžiagas.

Table of contents

List of figures

List of tables

Introduction

The physics of ionizing radiation and its effects on biological structures are known and well studied. Every moment, human bodies are bombarded with hundreds of particles of natural ionizing radiation emanating from space or the Earth. In addition to natural sources of ionizing radiation, countless artificial ones have been created, which, if misused, can pose a significant risk not only to human health but also to the surrounding environment as a whole.

To prevent or at least to know if an accident occurred, measurements like continuous background monitoring and identification of unknown radioactive materials are done, which are inherent subjects in the fields of radiation protection and medical physics. Measuring only counts of gamma photons, ionizing chambers like Geiger tube can be utilized, but to get the precise energy of gamma photon, detectors like proportional counters, solid-state semiconductor detectors or scintillating ones are being used.

These mentioned devices consist of many parts that need to work in unison, which leads to a highly complex system, and by extension making them difficult to understand how to use or fix, as well as it economical resources required to obtain such instruments.

Considering all the mentioned obstacles and difficulties “Do it Yourself” version of gamma spectrometer based on open-source principles would fulfill this missing piece in a whole variety of DiY tools and devices. Also, such devices would be helpful for citizen scientists to understand the basics of gamma spectrometry working principles, or even allow them to actually identify an unknown radioactive material.

Main aim:

Develop and test a gamma spectrometer based on open-source principles.

Tasks:

1. Analyze the principles of gamma spectrometry and available technical solutions;
2. Develop a prototype of an open source gamma spectrometer;
3. Perform functional testing and characterization of the developed device.

1. Literature review

Ionizing radiation is a flow of any elementary particle or electromagnetic wave that produces different signs of electric charges due to interaction with molecules or atoms in a substance [1].
The main types of ionizing radiation are:

- Gamma radiation;
- Alpha radiation;
- Beta radiation;
- Neutron radiation;
- X-Ray radiation.

One of the most measured radiation type is gamma rays. Gamma radiation is very high-power photons that are the product of gamma decay, and their energy typically varies between several keV up to approximately 100 TeV, depending on the nature of it [2]. Due to high permeability, gamma photons require a particularly dense, and with high linear attenuation coefficient material such as lead to stop them [3].
To be able to detect gamma rays, it must interact with matter, and that particular interaction somehow must be "seen". In the favor of how we understand the world, electromagnetic origin of gamma ray photon enables them to interact with electrons in the atoms of all matter. Three main processes that happen when gamma rays are going through medium are Compton scattering, pair production, and photoelectric absorption, more on them later [4].
Above mentioned processes also play the major role between quantum of gamma radiation and the detector medium. To be more specific, they directly affect the output of generated photons, electrons or electron-hole pairs which later are transformed by one way or another to the signal that can be converted to human readable form. Amount of generated charge carriers or photons depends on the total transferred energy to the detector; therefore, all the mentioned processes have specific features in the gamma ray spectra [5].

1.1. Gamma ray spectroscopy

Quantitative study which investigates gamma ray energy spectra is called gamma ray spectroscopy, and the device capturing gamma ray energy levels is known as gamma spectrometer. Gamma ray nature mostly comes from radioactive sources and their energies vary of material. Essential objective of gamma spectrometer is to "capture" gamma radiation photons, measure their energy, store that energy value in array, and later show how many times each energy level was recorded, in other words – pulse height distribution. Gamma rays have a peculiarity that it does not have charge, thus directly does not ionize, or excite atoms of the material it pervades [6]. This property makes measuring gamma rays energy one of the biggest obstacles, because when detecting, it is a must to ensure that high energy photon makes an interaction and transfers some or whole its energy to an electron of absorbing medium. Of many ways gamma rays can interact with matter, main three processes have significance in spectroscopy [7]:

- Pair production;
- Compton scattering;
- Photoelectric absorption.

1.1.1. Compton scattering

Compton scattering is described when a charged particle enters an atom, part of its energy is transferred to weakly bound outer shell electron, and it is kicked out. Due to conservation of energy and momentum only a partial energy transfer can happen, because electron is not able to absorb recoil energy. This process engages only the outer, least tightly, bound electrons of the atom [5]. The rest of the energy immediately exits the atom as a scattered photon with trajectory that is different than comparison to the one that it came from. It has less energy than the incident photon since part of it is "handed over" to the electron. The direction photon goes, to be exact – difference in angle between incident and final path, is proportional to the energy lost by the gamma ray and electron binding energy [8]. When the photon is only slightly deflected, small amount of energy is transferred to the weakly bound outer shell electron. Yet, if it is backscattered, it means that the maximum energy transfer occurred, so that direction of the gamma ray is reversed. All the possible angles of scattering can exist, which means that ejected electrons are produced with a continuum of energies, from almost zero to a maximum defined by the backscattering apex [7].

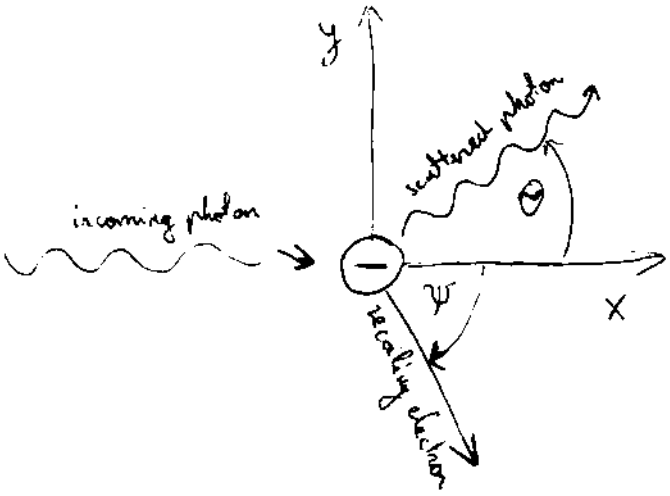

Fig. 1. Compton scattering

When detecting gamma rays Compton scattering, as mentioned above, produces all the possible energies which means it is difficult to relate this process to the energy of incident photon.
For example, taking the measurement of monoenergetic radioactive source – Cs^{137}, it has a full energy peak at 661.59 keV, which is formed when gamma photon gives up all its energy in the detector by a series of Compton scatterings which are followed by photoelectric absorption, or a single photoelectric absorption [8]. There is also a peak around 470 keV called Compton edge and it shows the maximum energy of a single Compton scattering that can be ceded to an electron by a 661.59 keV photon [5, 7]. This can be calculated using the following equation [8]:

$$E' = \frac{E}{(1+\frac{E}{m_0c^2})(1-\cos\theta)} \tag{1}$$

where E = photon energy before scatter; E' = photon energy after scatter; m_0c^2 = rest energy of electron = 511 keV; and θ photon deflection angle.

As can be calculated from equation above, another smaller peak, at ~180 keV is also present and is termed as a backscatter peak. It is formed when a gamma photon gets scattered by a large angle ~ 180° in a medium surrounding the detector and then absorbed by it.
As stated previously, gamma ray gives up most of its energy to the electron when it is scattered in the backward direction, yet some of the energy still remains. That photon with remaining energy can enter the detector back and interact with the detector medium, meaning it can be detected in the same way as an incident gamma ray, i.e., it will contribute to photopeak and Compton scattering distribution as well [7].
In conclusion, this process affects only the outer shell electrons, meaning nucleus has only a minor significance, so the possibility for this interaction is unrelated to atomic number. In other words, it mostly depends on electron density, which is nearly constant for all materials [8].

1.1.2. Pair production

When gamma ray interacts with an atom and incident photon energy is above 1.022 MeV, it is likely that in the field of a nucleus of absorber material the photon may disappear and be replaced by the formation of an electron-positron pair [5]. In order to conserve energy and momentum, this process only happens near the nucleus of an atom where strong coulomb force field is present. If gamma photon energy does not surpass 1.022 MeV, pair production cannot occur [8].

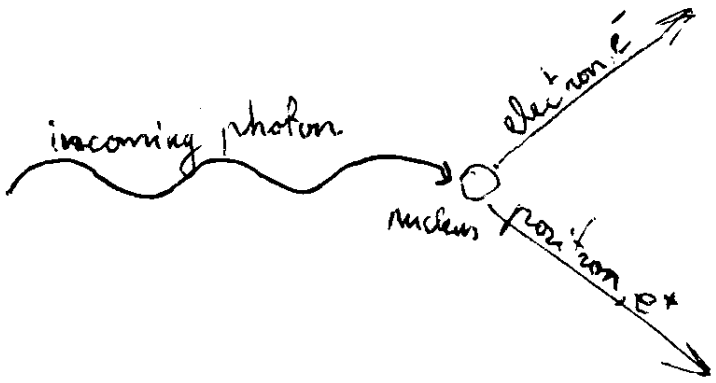

Fig. 2. Pair production

If it is exceeded, surplus energy comes out as kinetic energy that is shared between the electron and positron. Once the positron comes to the end of its track, it annihilates with an electron from the absorber, which produces two gamma photons of 0.511 MeV. Annihilation photon may undergo Compton scattering or photoelectric absorption interactions, contributing to single or double escape peaks, or may escape from detector [7, 9]. In case only one gamma ray escaped, single-escape peak 0.511 MeV below the photopeak energy peak can be observed, and double-escape one is double electron rest energy below. If the gamma rays are of very high energy, it might not be seen on the spectrum even though the escape peaks might be.
Pair production interaction process is negligible for nuclear material analysis because majority of signature gamma ray photon energies are below 1.022 MeV [9].

1.1.3. Photoelectric absorption

When a gamma ray interacts with an atom and it completely disappears, i.e., all its energy is given to one of the inner shell electrons of the atom, this process is called photoelectric absorption. Some of the gamma ray energy is used to overcome the electron binding energy, and most of the remainder is transferred to the freed electron as kinetic energy. Knocked out electron energy is equal to the incident photon energy minus its binding energy of atomic shell [5]. This process ionizes the atom, leaves it with a vacancy in a shell, which is filled after just a moment of time by an adjacent free electron. The energy of binding is not lost and appears as the photoelectron in coincidence with emitted characteristic x-rays [10]. Most likely for photoelectron to emerge is from the K shell due to typical, from a few keV for low Z materials to tens of keV for materials with high atomic number. Binding energy is freed in the form of Auger electron or a characteristic x-ray. This process is the predominant interaction for low-energy gamma rays, x rays, and bremsstrahlung [11].

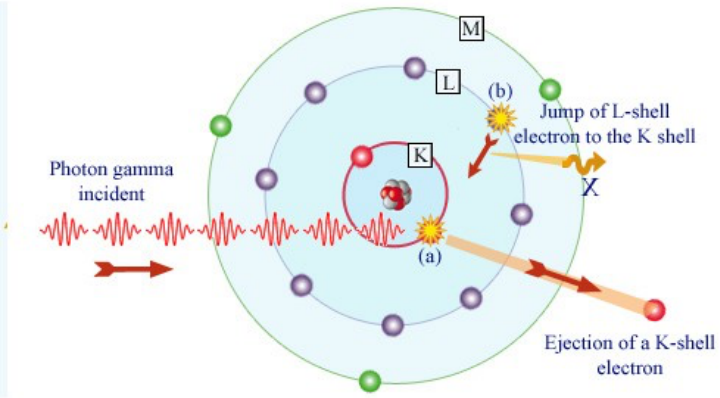

Fig. 3. Photoelectric absorption

Also, its importance is undisputed while detecting gamma rays because during liberation of photoelectron, which gives up most of a gamma ray energy together with one or more low-energy electrons, corresponds to absorption of the original binding energy of the photoelectron. Thus, if nothing escapes from the detector, the sum of kinetic energies that are created must be equal to the original energy of incident gamma photon [4].
Probability of this process depends on the atomic number, electron binding energy, and the gamma ray energy. The stronger electron is bound, the greater probability is [11].

1.1.4. Spectral features

Now that it is clear how a gamma ray interacts with matter, it is possible to sum up features of gamma ray spectroscopy in one picture. In figure 4 is a realistic representation of monoenergetic gamma-ray flux.

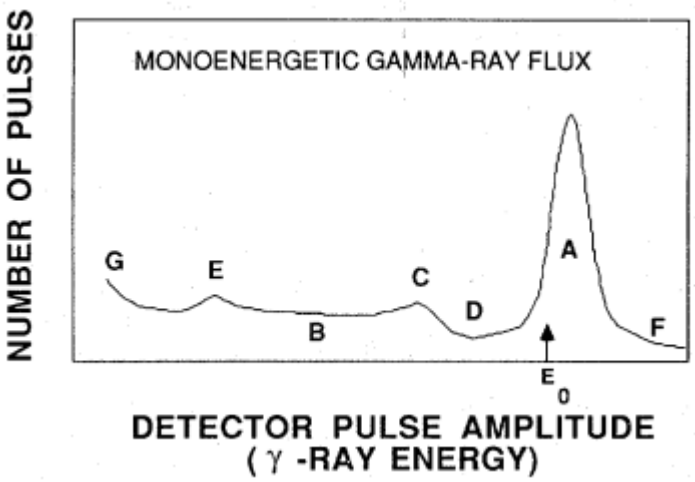

Fig. 4. Realistic representation of monoenergetic gamma-ray flux spectrum [11].

- A – Full energy photopeak;
  This peak shows the interaction between photon in detector via the photoelectric effect. All the photon energy is transferred to detector. To be more exact, most of the energy is transferred to photoelectron, which travels no more than a millimeter. The rest of the energy is carried off by an x-ray of Auger electron [11].
- B – Compton background continuum;
  This plateau is the result of interaction between incident gamma ray via Compton scattering. The energy varies according to the angle of scattered photon [5].
- C – Compton edge;
  This peak represents the largest energy of pulses in Compton scattering, this means that scattered gamma ray angle is 180 degrees. Compton edge is usually 200 keV to the left of photopeak [7].
- E – Backscatter peak;
  Part of gamma rays which undergo Compton scattering in the surrounding material will be scattered back to the detector. The majority of scattered gamma rays have an angle close to 180 degrees, but any photon scattered by more than 110-120 degrees, will have energies between 200 to 250 keV. Backscatter peak is asymmetrical, it has a tail to the right, which is the result of scattered photons at less than 180 degree angles [8].
- F – Excess energy region;
  This region in a monoenergetic source comes from high-energy gamma rays and natural background pulse pileup. Such thing occurs if the count rate is high enough [11].
- G – Low energy rise;
  Low energy rise is typically from electronic devices around the detector, because they usually produce low amplitude noise [5].

1.2. Gamma ray detectors

Three types of detectors are used to measure energy of the gamma photons:

- Proportional detectors;
- Solid-state semiconductor (SSS) detectors;
- Scintillation detectors.

In both proportional, and SSS detectors the incident radiation directly affects gas or material, and sets free some charge carriers which are between two electrodes. Where in scintillation detectors, incident radiation energy is transformed to light photons, which are later caught in photomultiplier tube.

1.2.1. Proportional detectors

Proportional counters are gaseous type ionization detectors. They use a combination of Geiger-Muller tube and ionization chamber mechanisms. In other words, detector is a chamber filled with inert and quench gas mixture. When ionizing particle enters the chamber, it hits atoms of the inert gas, ionizes it, and produces electrons and positive ions – ion pairs. Such pairs start Townsend avalanches. Proportional counter name comes from phenomena, that concrete amount of energy of primary ionizing particle produces concrete amount of ion pairs. In such detectors, typically, 30,000 ion pairs are created from 1 MeV particle [12].

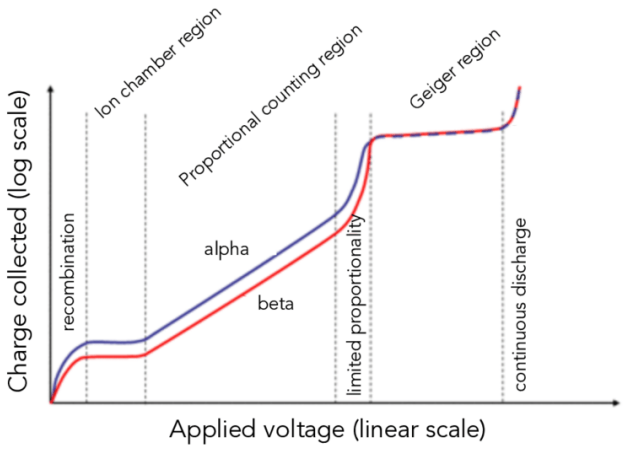

Fig. 5. Regions of gaseous ionization detector [12]

Main aim of proportional counters is that every ionizing event should produce one and only avalanche [13]. This ensures proportionality between total ion current and original ionization count. To achieve proportionality, geometry of the tube, voltage between electrodes, and diameter of the positively charged wire inside chamber, are essential to ensure [12]. Applied voltage to the detector is adjusted in such a way that the conditions correspond to the proportional area (figure 5). Main disadvantage of proportional counters is that it requires extra precise and stable power supply and amplifier, to make sure the operating conditions are between proportional counting region.

1.2.2. Solid-state semiconductor detectors

To measure the impact of incident charged particles or photons, SSS detector utilizes silicon or germanium [11]. When ionizing radiation hits detector, it sets free some charge carriers which are between two electrodes. It produces holes and free electrons, where number of ion pairs are proportional to the energy of the radiation to the semiconductor. Because of that, some electrons are transferred to the conduction band, and same number of holes are created in valence band. Between the electrodes there is an electric field, so both electrons and holes travel to electrodes, where they produce measurable pulses [14].

Fig. 6. Solid-state semiconductor detector [15].

In semiconductor, it is always known what amount of energy is necessary to make an electron and hole pair, so measuring how many pairs incident radiation produced it is possible to know the incident energy. The biggest drawback of semiconductor detectors is its price, e.g., used Germanium semiconductor detector costs starts from 12,000$ [15]. Also, it must be cooled with very low temperature materials like liquid nitrogen to operate without any noise.

1.2.3. Scintillation detectors

One of the oldest techniques for detecting ionizing radiation is by using scintillation light. It is still the most used method for spectroscopy and detection of wide range of radiations. As mentioned before, scintillation detectors consist of two main parts. Scintillating crystal and device for collecting light photons [5]. Scintillators can be of two types – inorganic and organic ones.

The ideal scintillation material should have the following properties:

- Converting kinetic energy of incident radiation to longer wavelength photons, and should be highly efficient;
- Conversion should be linear/proportional over as wide range as possible;
- Material should be transparent to the wavelength of its own emission for good light collection;
- Short luminescence time for fast signal pulses;
- Refraction index should be near glass one, to let to couple as efficient as possible the scintillation light to a light sensor;
- Medium should have a good optical quality and be easy to manufacture in sizes of around 3 by 3 centimeters so could be used practically in the detector.

Yet, no scintillating material meets all these criteria, and the choice is always about finding a middle ground betwixt these factors. Most practiced scintillators are alkali halide crystals, of which sodium iodide is the front-runner, due to the greatest linearity and light output, nevertheless it has quite slow response time [16]. Liquids and plastics are popular choice if selecting from organic scintillators, they are faster, however produces less light [17]. Also, since the field that scintillators are used is usually gamma spectroscopy, inorganic crystals are preferred because of high Z value and high density, it

allows the gamma-ray to interact with earlier mentioned processes much better with the crystal medium. Though, organics are great for beta or fast neutron detection due to hydrogen content [18]. Meanwhile, solid-state semiconductor detectors are much more sensitive, have better resolution than scintillation detectors, and suit much better for the unknown radionuclide determination, they are still not so popular as scintillating ones.

One of the main drawbacks of SSS detectors is that they can function only in the environment of very low temperatures, to be more exact, they are cooled with liquid nitrogen, otherwise a lot of noise is generated due to thermal excitement of electrons into the conduction band. Nonetheless, to have a similar stopping power as a normally used scintillating crystal, such detectors become very expensive to manufacture, thus will not be analyzed any further. As well as proportional counters, they require very stable environment and expensive equipment [19].

1.2.3.1. Organic scintillators

Working principle of fluorescence in organic scintillators originate from transitions inside the single molecule energy level structure, to be exact π-electron structure. As can be seen in figure 7, energy can be absorbed by exciting the electron configuration into any of the excited singlet states – S1, S2… Typical energy spacing between energy levels is ~ 1-2 eV, where between vibrational states of the molecule energy difference is the order of 0.15 eV. Due to large spacing between vibrational and thermal energy spaces, nearly all molecules are in the ground (S00 state) [20].

When incident radiation passes through medium it can either excite electron level or vibrational level. Arrows pointing up in the figure 7 shows molecule's energy absorption. Excitations which can be seen for singlets are de-excited in picoseconds to the S1 state through internal radiationless conversion. Then electron on S1 state decays to the ground S0 and emits a scintillation photon. It decays to ground level because surplus vibrational energy, like in S11 or S12, is not in thermal equilibrium with the other singlets around, thus it quickly loses it [21].

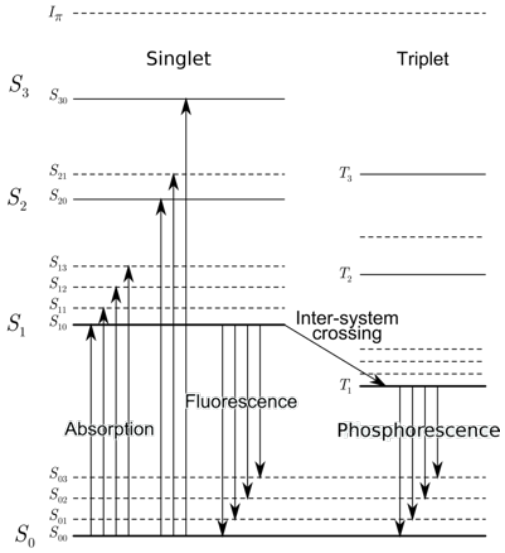

Fig. 7. Occurring processes in organic scintillators [21]

Lifetime of the triplet state is longer than of the singlet one. It is due to conversion called inter-system crossing. Some of the excited singlet states can be transitioned into triplet states. Existence of T1 can be as much as millisecond, where in a de-excitation from T1 to ground state – S1 means it was a delayed light ejection called phosphorescence. Since T1 is below S1, wavelength of phosphorescence will be longer than for fluorescence [21].

The more energy is converted into visible light from the incident particle energy, the greater the scintillation efficiency is, but this phenomenon is not always desired. High scintillation efficiency has a drawback because de-excitations which do not engage emission of light mainly involves degradation to heat. All the radiationless de-excitations are named as quenching. Also, it is a must to eliminate impurities, like dissolved oxygen inside the crystal, which deteriorate light output and is considered as a component of quenching as well.

1.2.3.2. Inorganic scintillators

Mechanism of scintillation in inorganic material is based on the energy states of the material crystal lattice. As can be seen in figure 8, electrons can only be in a discrete energy bands. In valence band electrons are bound to crystal lattice, where in conduction band they have enough energy to go throughout the crystal. Inside the third – the forbidden band, electrons are never found in pristine crystals.

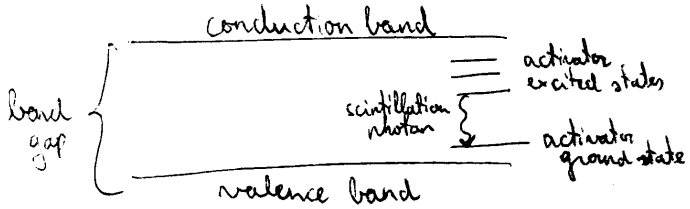

Fig. 8. Occurring processes in inorganic scintillators

Thus, absorption of energy in pure crystals can happen and electrons from valance band get elevated into conduction band, this process is very inefficient. On top of that, typical range between the bands are such that it would be too high for the photon of the visible wavelength.
To increase visible photon emission probability, small impurities are added, which are called activators. It creates special sections inside the lattice which lets electron to get stuck somewhere in between valence and conduction bands. Since the required energy is lower on the activator excited state, de-excitation also emits a photon with lower energy, meaning it is probably in a visible spectrum. Sites where de-excitation happens are named luminescence or recombination centers [22].
When incident particle passes through inorganic scintillator medium, it creates many electron-hole pairs between valence and conduction bands. Because ionization energy of impurity, i.e., activator, is lower than the lattice, the positive hole will ionize the impurity, leaving the electron to freely mitigate throughout the crystal. This allows free electron to drop inside the impurity site and create neutral configuration with its own array of excited energy states showed in figure 8. De-excitation will ensue and very quickly if the state that is formed inside activator is allowed to transition. Emitted photon wavelength depends on the selected impurity that is added to the crystal and time of de-excitation is between 50-500 ns. This time value is called decay time, which is one of the main properties to look into when choosing a crystal [23].
Same as in organic crystals, the main process of producing light photons is its own enemy, due to probability that state formed inside activator can have configuration that de-excitation is forbidden. Such issue requires additional energy to raise the state until it is possible to transition to ground state. Thermal excitation is one of the sources of this energy, which results slowing the light and is called phosphorescence. It is a significant component of “afterglow” in scintillators. Quenching is also possible between some of the activator excited states and ground state, which does not produce visible photons [22, 23].

Scintillation process efficiency is determined on calculating how much energy is required to generate one electron-hole pair. On average, for a broad range of materials it takes around three times more than the bandgap energy. As an example, for sodium iodide crystal about 20 eV have to be taken from incident gamma ray to produce single electron-hole pair. Meaning typical gamma photon from ^{137}Cs with 661.59 keV creates about 3.31×10^3 electron-hole pairs inside such crystal [5].
Another thing that must be considered is that crystal can absorb the light that was produced by itself. When almost the same amount of energy is liberated, and when an electron-hole pair recombines as it is needed to excite it, self-absorption will happen due to absorption, and emission spectra will overlap. However, inside the crystal with added impurities, i.e., activators, emissions arise from the activator site, meaning transition energy is lower than the electron-hole pair excitation energy. As a result, emission spectrum has less energy, so longer wavelengths, and will not be altered by the absorption of the crystal.

1.3. Photomultipliers

Since solid-state semiconductors and proportional counters were ruled out, for the second part of scintillation detector device to catch produced light photons is needed. Two types of light sensors are being usually used:

- Photodiodes;
- Photomultiplier tubes (PMTs).

These devices convert light photons to an electrical signal, yet have their own merits and demerits. For example, photodiodes, small semiconductor devices which have a very thin layer of silicon where light is absorbed and produce electron-hole pairs. However, the charge is not amplified, which makes photodiode very sensitive to electronic noise, since the output amplitude is quite small. It has an advantage of high quantum efficiency, but it does not outweigh the noise sensitivity.
Another type, photomultiplier tubes, are also being used together with scintillating crystals, and are more popular than photodiodes, due to its high signal amplification. This amplification requires high voltage power supply, up to 1.5 – 2 keV, but still in practice it is considered to be a better solution [24].

1.3.1. Photomultiplier tube

Photomultiplier tube (PMT) is a vacuum tube which has an input window, photocathode, focusing electrode, dynodes and finally an anode [25]. Its principal construction scheme is shown in figure 9.

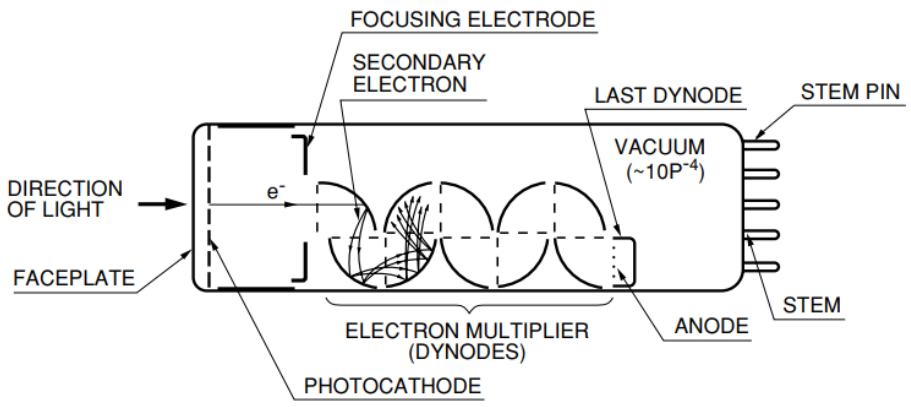

Fig. 9. Principal construction scheme of photomultiplier tube [25]

When light hits photomultiplier tube, photocathode converts that photon into an electron. Electron emitted from photocathode enters vacuum where it first meets focusing electrode, which directs electron onto first dynode in dynode array. Each dynode has higher potential difference to ground than the one before and the electron is accelerated from 1st to 2nd and so on, until it reaches the anode. When electron hits first dynode, it produces more electrons which are accelerated to the 2nd dynode. Then, each electron that is collected on the dynode transfers its energy and excites more electrons, this way they are multiplied. In the end each electron is collected on the anode and signal is acquired [26].

1.3.1.1. Photocathode

First component of PMT that light meets is photocathode (PC), where the photon energy from scintillating crystal is transferred to electrons inside PC. This effect is called photoelectronic emission. Photocathodes can be of two types, which describes their photoelectron emission process [25]:

- Transmission mode;
  Usually, transmission mode PCs are just a glass plate on which thin film is deposited. Photoelectrons are emitted in the same direction as the incident light hit it. Used for head-on PMTs, which have a window at the end of a tube, like in fig 9.
- Reflection mode;
  Made of metal plate and photoelectrons are emitted opposite way than the incident photon. Used mainly for side-on PMTs which have a window on the side of the glass bulb.

Since PC is a semiconductor, band model could be used to describe its working principle.

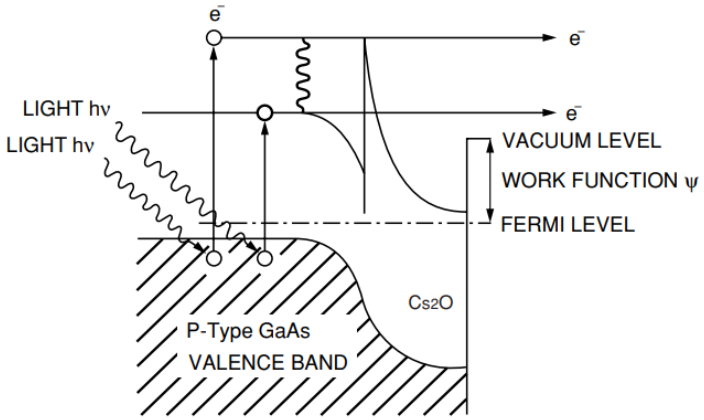

Fig. 10. Band model of semiconductor photocathcode [25]

As can be seen in figure 10, there is a forbidden-band gap that electrons cannot occupy, also interval between conduction band and vacuum level, and work function describing energy difference between Fermi level and vacuum level. When the photon hits a photocathode, electrons that are in valance band absorbs photon energy and gets excited. Excited electron then moves towards the photocathode surface and if it has enough energy to overcome vacuum level barrier, it is emitted from PC as photoelectron. This process can be expressed in a probability process and quantum efficiency, i.e., ratio of output electrons to incident photons is given by equation 2 [27]:

$$\eta(v) = (1 - R)\frac{p_v}{R}.\left(\frac{1}{\frac{1+1}{kL}}\right).p_s \quad (2)$$

where R – reflection coefficient, k – full absorption coefficient of photons, P_v – probability that absorbed photon excites electron to a greater than vacuum level, L – mean escape length of excited electrons, P_s – probability that electrons which reached photocathode surface may be released into vacuum, v – frequency of light.

Now that electron nature in PMT is explained, its path along whole tube must be described.

1.3.1.2. Electron path in PMT

At first, when electron just escaped PC, it is affected by magnetic field of focusing electrodes (FE), it makes sure the electron hits the first dynode and does not fly somewhere else. Since this is a crucial part of PMT design itself, when constructing a new tube, PC shape (planar or spherical), shape and arrangement of FE, and supplied voltage must be considered. Main aim is to efficiently focus electron onto the first dynode [5].

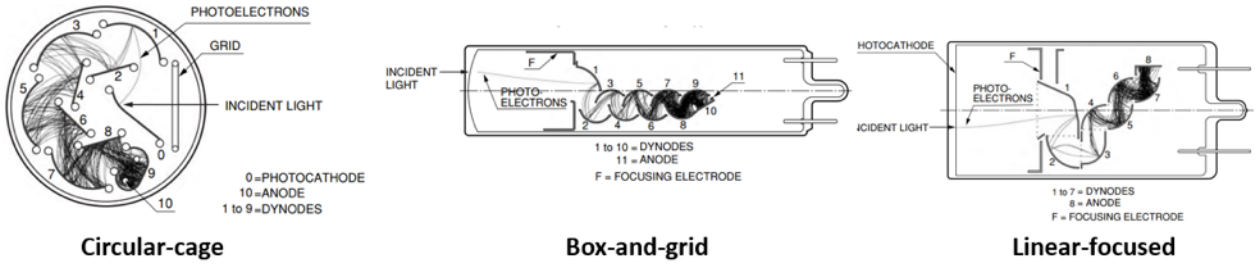

Fig. 11. PMT dynodes arrangement types [28].

Dynode section is usually constructed from a few to more than twelve stages of dynodes which have curved surface. For enhancement of collection efficiency of each dynode and minimization of electron transit time spread, optimal arrangement and configuration should be determined from analysis of electron trajectory. It must be placed in such way that it prevents ion or light feedback from the latter stages. Most popular arrangement types are circular-cage, box-and-grid, and head-on structures, which are shown in figure 11 [25].

1.3.1.3. Dynode array

As mentioned above, potential distribution and electrode structure of PMT is designed to provide optimum performance. Photoelectrons are multiplied by first through the last dynodes, where current can usually be amplified from 10 to as much as 10^8 times and are finally collected on the anode.
Mostly dynodes are made of nickel, stainless steel or copper-beryllium alloy and usually coated with secondary emissive material like alkali antimonide, beryllium, magnesium oxides, gallium or gallium arsenide phosphides.
When primary electron hits first dynode's surface, k amount of secondary electrons are produced. This number k is called secondary emission ratio and it varies of material and accelerating voltage of primary electron.

Conventionally, current amplification, or in other words – gain, of a PMT with n number of dynodes and average secondary emission ratio k per stage is described as k^n [5].

1.3.1.4. Anode

Anode design must be chosen thoughtfully, because its shape must be optimized so that electron trajectories do not miss it. Commonly, anode has a form of a plate, rod or mesh electrode. Most important factor when designing an anode, it must be able to establish an adequate potential difference between last dynode and itself and prevent space charge effects and obtain large output current [25].

1.4. Scintillation detector characteristics

1.4.1. Energy resolution

In the gamma spectroscopy measurement, the pulse heigh discrimination is a crucial part in determining photoelectric peaks and result chiefly depends on this part. This process is named as pulse height resolution or energy resolution [11].
It is defined using the following equation and data from figure 12.

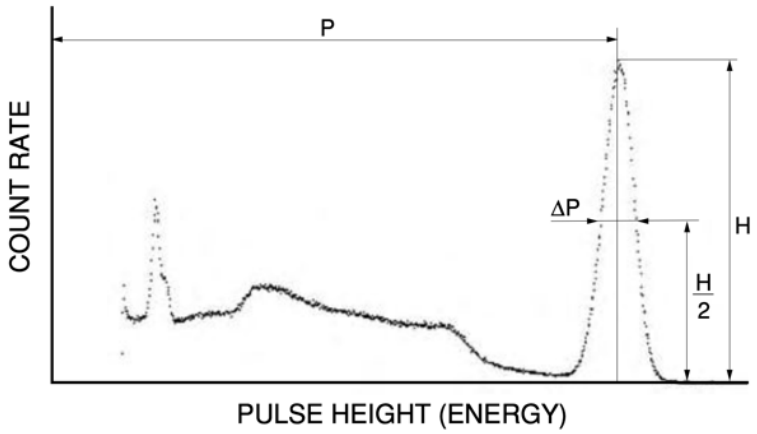

Fig. 12. Definition of energy resolution [11]

$$R = \frac{\Delta P}{P} \tag{3}$$

where R is energy resolution, P – peak value, ΔP – full width at half maximum (FWHM).

Factors that contribute the most to the energy resolution [18]:

- The scintillator's energy conversion efficiency;
- The scintillator's intrinsic energy resolution;
- The PMT's light collection efficiency;
- The PMT's photocathode quantum efficiency;
- The first dynode's collection efficiency;
- The tube's multiplier section fluctuations;

1.4.2. Time

The photomultiplier tubes have an exceptionally fast time response, which corresponds to the time, required for the photoelectron, that is emitted from the photocathode, to reach anode after being

multiplied. As it was mentioned before, the biggest impact on transit time has the dynode type but increasing supply voltage also helps to improve the time response [25]. Typical time characteristics based on dynode type provided by Hamamatsu can be seen in table 1.

Table 1. Typical time characteristics for different PMT dynode arrangements [25].

Dynode Type	Rise Time	Fall Time	Pulse Width (FWHM)	Electron Transit Time	TTS
Linear-focused	0.7 to 3	1 to 10	1.3 to 5	16 to 50	0.37 to 1.1
Circular-cage	3.4	10	7	31	3.6
Box-and-grid	to 7	25	13 to 20	57 to 70	Less than 10
Venetian blind	to 7	25	25	60	Less than 10
Fine mesh	2.5 to 2.7	4 to 6	5	15	Less than 0.45
Metal channel	0.65 to 1.5	1 to 3	1.5 to 3	4.7 to 8.8	0.4

1.4.3. Linearity

Cathode linearity mostly depends only on a photocathode material, which is not possible to tweak without changing the tube, but anode linearity is a completely different story.

The anode linearity is defined by two factors: space charge effects, and voltage-divider circuit. Regarding space charge density, it is largely dependent on the current of the signal peak. When a large current is produced by the intense light entering a photomultiplier tube, it increases the space charge density, especially in the latter dynode stages. It also causes current saturation [29].

Space charge effect also depend on the intensity and electric field distribution between each dynode. As mentioned before, dynodes are situated carefully to provide higher electric field strength, as well as dynode area is specifically large so that density of the signal is lower per unit area. Meaning, the more the electric field strength, i.e., potential difference, is increased, the better linearity can be seen [30].

Another solution to improve pulse linearity is modifying voltage divider. Enhancing the interstage voltages at the latter dynode stages helps to keep optimum electric field distribution, this voltage divider adjustment is called “a tapered” one.

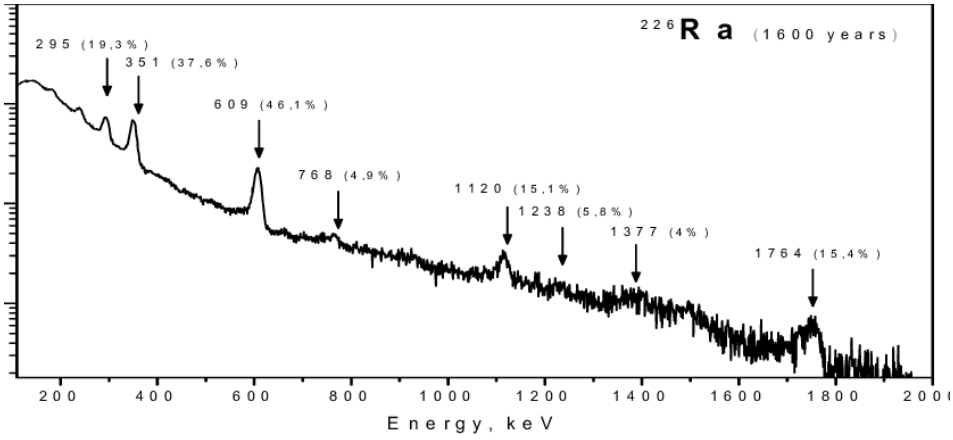

Fig. 13. Spectrum of ^{226}Ra [31].

^{226}Ra is good radiating source to make a measurement of detector linearity since it releases range of products between 10.8 keV to 2.2 MeV. From such measurement it should be expected to see a consistently declining line with peaks according to the energies of ^{226}Ra [31].

1.4.4. Uniformity

Uniformity of PMT is the output signal variation when incident light photon hits different location of the surface of photocathode. It is a significant characteristic for circular cage, box-and-grid or side-on tubes. Gamma cameras which are used for medical diagnosis demand a good position detecting ability and uniformity is an important parameter. Thus, in gamma spectroscopy, head-on type is the most popular, in which photocathode uniformity plays a minor role. However, light entering the photocathode should focus to the very middle, because on the sides the performance of photocathode decreases, since it is much harder to focus the photoelectron onto the first dynode if it is produced near the side wall of the tube [5, 25].

1.4.5. Stability

Current output may vary due to “life” or “drift” characteristics, as well as “fatigue” caused by the stress of current, ambient temperature, and voltage supply. These instabilities should be considered when doing short or long measures with the PMT, because the sensitivity of the cathode of PMT shows good stability even after long operating time. Life and drift indicate the extent of gain variation with operating time, to be more exact, it chiefly depends on variations of secondary emission ratio [5].
Keeping signal output current as low as acceptable, within a few microamperes, is recommended. It is so because life and drift characteristics depend on the magnitude of the output current. As well as applying the power supply voltage to the PMT or aging it prior the usage, to ensure it is more stable. In applications where output stability within a few percent is required, aging or warm-up is recommended.
Aging is when PMT is continuously operated from few to tens of hours, but not exceeding the maximum rating of anode output current. This process helps to stabilize the drift, also, if tube is warmed up before the usage, the drift will be further stabilized [25].
To achieve stable operation of PMT, it is recommended to warm it up for about 30 – 60 minutes. It should be especially done when it is used for the first time. Warm up can be shortened after a long period of operation, as well as with higher anode current. Usually, it is performed for 20 – 30 minutes at a supply voltage near the actual operating voltage, but if PMT is operating in a low current environment, warm-up should be done applying working voltage and should last for about one hour [29].

1.4.6. Dark current

When PMT is operating, even in a completely dark state, small amount of current still flows, which is called dark current. Since PMTs are used to detect very small amounts of light photon pulses, this current must be kept as small as possible.
Main causes of the dark current [32]:

- Thermionic emission;
- Ohmic leakage between electrodes;
- Field emission;
- Ionization current from residual gases;

– Noise caused by cosmic rays or environmental gamma rays.

Dark current is enhancing together with increasing supply voltage, but the rate of increase is not constant, it can be seen in figure 14.

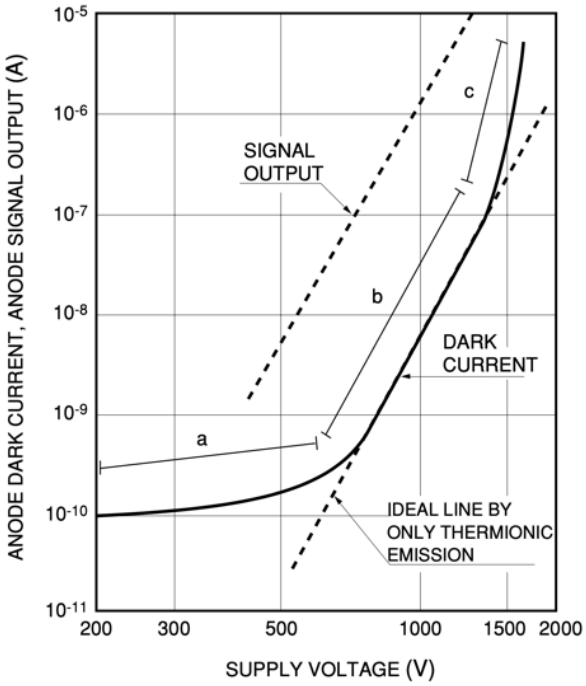

Fig. 14. Typical dark current vs. supply voltage characteristic [25]

where *a* region corresponds to low voltage region, *b* – medium and *c* to a high voltage region. Each of regions are dominated by different processes, low voltage one is mostly leakage current, *b* – by thermionic emission, and high voltage region by the field emission.

1.4.6.1. Thermionic emission

Due to very low work function of photocathode and dynodes, event at room temperature, they can emit thermionic electrons. It was studied by W. Richardson and he derived an equation that describes this process: [33].

$$i_s = AT^{\frac{5}{4}} e^{\frac{-e\varphi}{KT}} \tag{4}$$

where A – constant, T – absolute temperature, e – electron charge, K – Boltzmann constant and Φ – work function

From the equation above is apparent that decreasing temperature will decrease dark current as well, which is an effective technique to reduce it. However, this effect becomes limited when dark current reaches a level where ohmic leakage starts to dominate.
Although, thermionic emission arises from photocathode as well as from dynodes, the one from photocathode play a major role on the dark current. It is so, because dynodes contribute much less to the output current, especially on the latter stages, but also, due to the size difference – photocathode is larger in size than each dynode.

1.4.6.2. Ohmic leakage between electrodes

Usual voltage applied to PMT is from 500 volts up to 3000, yet it handles very low currents which are in a few tens of microamperes at maximum. When such high voltage is applied, insulating material quality used in the tubes is very important. Leakage current is determined from the Ohm's law, meaning it is always there when PMT is used, but it has less effect on the dark current in normal operating conditions.
A leakage current can be generated between the last dynode and the anode inside the tube, also due to bad insulation of base and glass stem, or between the socket pins itself. PMT surface, i.e., glass stem, socket, or base, should be kept clean because moisture or even dirt that is conductive can increase the ohmic leakage [11]. If it happens that the tube gets contaminated, it is recommended to clean it with isopropyl alcohol, yet photocathode should be cleaned only with water, to not damage thin layer that is coated [25].

1.4.6.3. Field emission

Electrons can be emitted from dynodes due to electric field strength if PMT is operated at an exaggerated voltage. In the sequel, the dark current increases precipitously. This process can be seen in the figure 14 in region *c*. The maximum tube supply voltage must not be exceeded, because field emission shortens the life of the PMT. It is recommended to keep the voltage 20-30% lower than maximum recommended rating [5].

1.4.6.4. Ionization current from residual gases

PMTs are vacuum tubes, so the inside of it, the vacuum is around 10^{-6} to 10^{-5} Pa, but even in such environment, there are still some remaining gases that cannot be ignored. These residual gases may be ionized during high current operation, and it can result in a noise pulse, which usually comes just after the main photocurrent. Such pulses are called afterpulses and can easily cause an error during gamma spectroscopy measurement [5].
When positive ions return to the photocathode, they produce photoelectrons which result in afterpulses. The amplitude of such afterpulses depends on a position where they are generated and what type of ions are recombining. Time delay from the actual pulse can range from a several hundred nanoseconds up to a couple microseconds [21].

1.4.6.5. Noise caused by cosmic rays or environmental gamma rays

Many types of cosmic rays are always hitting earth. One of them is muons, which are the major component of this PMT noise, since Cherenkov radiation may occur when they pass through the glass envelope, large number of photons are released.
Another source of noise can occur from gamma/beta emitter – ^{40}K, which is usually found in glass as potassium oxide (K_2O). Furthermore, gamma photons that are emitted from environment around the detector can be another issue [29].
However, these dark noises are quite negligible since they occur much less frequently and can have a noticeable effect on very low count measurements.

1.4.7. Housing of photomultiplier tube

As discussed before, PMT should be kept clean from environment contamination, as well as from physical damage. However, there are three more factors that PMT should be shielded from [5, 25, 29]:

– Light;
– External electrostatic fields;
– External magnetic fields.

1.4.7.1. Light shield

Photomultiplier tube is a very highly sensitive photodetector, which is able to detect extra low light levels, meaning, during the measurement, it should be kept in a place where no extraneous light can enter.
Usually, leakages occur though the connector of signal cable or mounting or screw holes, as well as through seams in the housing itself. To prevent unwished light to reach PMT, using black silicone rubber can help achieve it. Also, to fill any gaps around attached components, usage of O-ring or black soft tape is highly recommended. The last thing, if light somehow got inside, coating the inside of the housing with highly light absorbent material will prevent light scattering or reflection [5, 34].

1.4.7.2. Electrostatic shield

The housing of PMTs is usually made of aluminum, and during the measurement it is kept ground potential, which helps to shield the housing from external electrostatic fields. Extra care must be taken that there are no contact between the tube and the housing because any object brought close to the bulb with ground potential will cause noise. Housing and PMT must have a sufficient separation [25].

1.4.7.3. Magnetic shield

PMTs are especially sensitive to a magnetic field and even terrestrial magnetism influences the performance of the tube. Unfortunately, unlike the electrostatic shield, there are no magnetic flux conductors, thus, it is not possible to completely shield something from magnetic field. Most common technique to reduce the effect of an external magnetic field is wrapping PMT with high permeability metal, but still, it does not block all the magnetic field.
In normal environment, i.e., not in a high magnetic field, it is not required to have a housing from high permeability material, and “permalloy” is widely used [5. 29]

1.5. Compulsory equipment for scintillation detector

1.5.1. High voltage power supply

Another crucial part of scintillation detector is the high voltage power supply (HVPS) to drive the PMT. To be able to provide required potential difference for each dynode, that it would be able to accelerate the electrons to vital speeds, power supply that can provide at least 500 volts must be used, and its potential must be distributed to each dynode accordingly [35].
To select appropriate HVPS, parameters such as current output and high voltage output must be considered, also it is not enough just to achieve high voltage, but it is requisite to keep it stable. Since gain of PMT is extremely high, tubes are very susceptible to variations of voltage. HVPS stability must be held within 0.1 percent [25].
There are two types of HVPS available, modular ones or bench-top supplies. Each type has its own merits and demerits. Modular power supplies are mostly used inside a complete circuit, like in a complete product of a detector and are selected for exact PMT, where bench-tops provide more variations of voltage and current output, but mainly used, as its name suggests, on a bench in the laboratory.

a *b*

Fig. 15. High voltage power supplies, bench top (*a*), modular (*b*) [36].

Voltage divider

To operate PMT, as stated above, high voltage is applied across cathode and anode, with a proper voltage gradient between each dynode [37]. This voltage gradient can be made using multiple independent HVPS, but such approach is not practical at all. This is where voltage divider circuit comes into play.

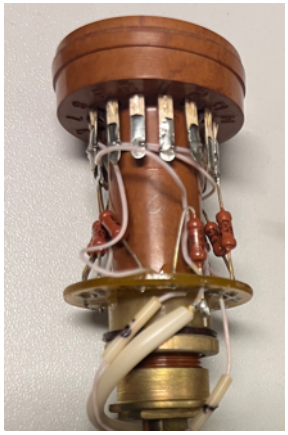

Fig. 16. PMT socket with voltage divider

Voltage divider referenced to ground is created by connecting two or more electrical impedances in series. This phenomenon could be explained as an example with two resistors: when two resistors are connected in series, same value of electric current must flow through each of it, since current has nowhere else to go, thus providing a *current · resistance*, voltage drop across each resistive element can be seen.

With a supply of voltage V, Using Kirchhoff's Voltage Law together with Ohm's Law, voltage dropped across each resistor can be found with derived equation [5]:

$$V_{R_n} = V_s \left(\frac{R_n}{R_a + R_b + \ldots + R_k} \right) \tag{5}$$

where V_{Rn} – Voltage at R_n resistor, $R_{a\ldots k}$ – resistance of other resistors in circuit and V_s – voltage of power supply.

Example of implementation of the voltage divider is shown in figure 16. PMTs always have the pins which are connected to each dynode. These pins are directly connected to the voltage divider which can be constructed in 3 different types [38]:

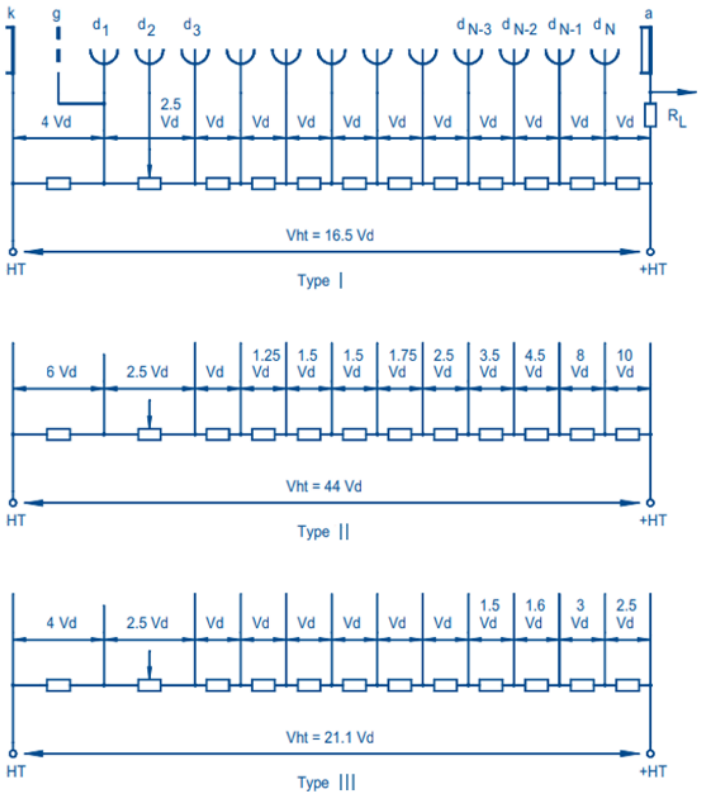

Fig. 17. Voltage divider types, where V_d is smallest inter-dynode potential [38]

- Type I;
  Same voltage for all multiplier stages, except for first few. This distribution gives highest signal gain for a set supply voltage and is particularly suitable for nuclear spectrometry applications.
- Type II;
  Progressive voltage distribution, increasing value of each resistor from cathode to anode. Such approach provides highest linear peak current, but gain is much lower than type I distribution.
- Type III
  In between type I and II, this distribution provides acceptable gain and gives bearable linearity. Usually, this type of set is used in physics experiments requiring accurate timing combined with ability to analyze pulse heights over a wide dynamic range.

When designing a resistive voltage divider, it is a must to keep in mind supply voltage, distribution type, and anticipated mean anode current I_a. To assure that voltage variations due to anode current variations are negligible, normal divider current – I_d, must be much larger than I_a. Great rule to follow is [25]:

$$\frac{I_d}{I_a} \leq 100 \tag{6}$$

Sometimes, when anode current can reach high values for only a small fraction of the time, it is recommended to connect reservoir, in other words – decoupling, capacitors to the dynodes. Charge stored by the capacitors must be sufficiently large compared with that supplied by each dynode when

pulses pass through the tube, so that the dynode potentials will not vary by more than one or two volts [25, 38].

Decoupling capacitors

Provided the dynodes are sufficiently decoupled, rising values of current in pulse operation could greatly exceed the mean value of the divider current. To remember equation 6 rule, value of I_a should be the mean anode current based on the anticipated pulse amplitude and duty factor. To restore the charge transferred by pulses passing through the tube, capacitors may be places in series or parallel to the dynodes [5, 38].

1.5.2. Multichannel analyzer

The amount of charge in the pulse produced by the PMT is proportional to the energy of incident ionizing radiation energy. At first, to prevent wasting processing time on the noise, MCA uses comparator with its voltage threshold set just above the maximum amplitude of the noise. When valid pulse from PMT exceeds the threshold voltage, following circuitry is triggered to search for the maximum height of the pulse. That maximum pulse heigh is presented to an analog-to-digital converter (ADC) so that it is "translated" to a digital representation of the analog voltage [39]. Fundamentally, ADC compares the analog pulse height to a ladder of voltage levels. The ladder usually exceeds from 0 to 5V with a uniform space between the rungs, where each of it represents a defined voltage. When a pulse arrives, ADC's job is to look at that voltage of the pulse and decide between which two rungs it belongs. Later, depending on a device, this digital value is passed to an interface of choice [40].

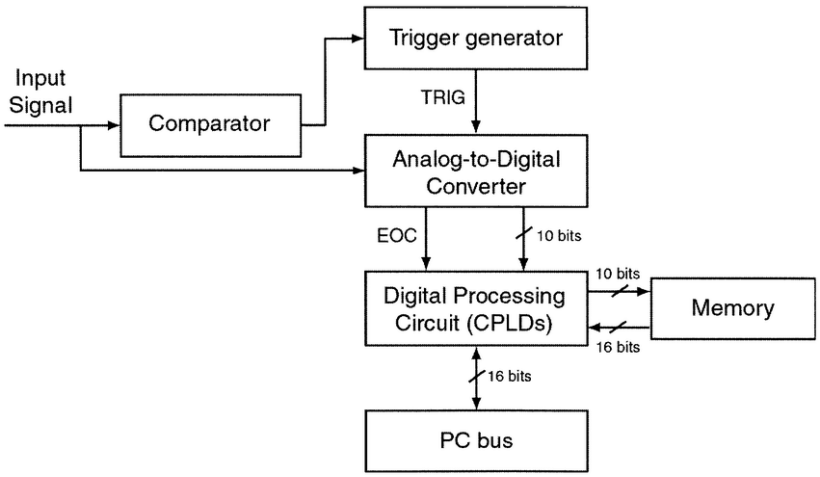

Fig. 18. Principal scheme of multichannel analyzer [40].

1.5.3. Processing of MCA signal

Once digital value of an analog pulse is acquired, it can be processed in various ways. Nowadays most common technique is to use personal computer which has an operating system in it. In this method digital signal is passed to an integrated circuit which is recognized as an external sound card and communicates with PC through an USB interface. This way computer understands a signal as continuous "sound" which can be easily manipulated and analyzed with the help of open-source software. "PRA" is one of the most popular choices to perform spectral analysis. At first, this software receives digital values of signal from PMT and stores each pulse value in memory. If the same value

occurs twice or more, it adds a count to that value. Besides acquiring and counting pulse values, additional filtering can be used to get better results. During the data collection, histogram is shown, which shows spectrum of energy levels, yet it does not mean that results are reliable out of the box, since parameters like bin size or pulse shape must be set. Selection of these parameters will be covered in methods section [41].

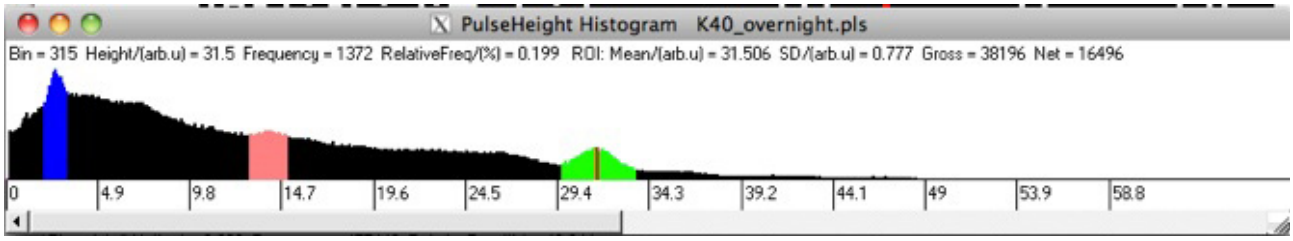

Fig. 19. „PRA“ for visualization energies spectra of gamma rays [41].

1.6. Radiation safety

Radiation safety is a very broad topic, which includes radiation detection, but this itself is very wide as well, mostly it is about continuous environment monitoring, identification of unknown materials or checking how much radiation dose was received per amount of time in hazardous place.

Continuous environment measurements sometimes employ simple Geiger counters, due to its low cost and easy operation. Such devices are detecting gamma rays in the air, and usually placed in various places, but mostly around objects that can release gamma radiation to environment. Such detectors are also used as personal handheld radiometers, for example when exploring a forest near the NPP, it can instantly show increased contamination [42].

Also, gamma spectrometers are not the exception for continuous environment measurements. Lithuania has the radiation monitoring network called RADIS. RADIS is an early warning system for radiation hazards consisting of ambient dose rate stations. It currently has 43 stations measuring the level of ionizing radiation in the environment (ambient dose rate) across whole country [43]. It employs 12 gamma spectrometers “SARA” made by “ENVINET GmbH” [44]. “SARA” detectors are based on NaI(Tl) scintillating crystals, and can detect particles from 30 keV to 3 MeV. Also, according to manufacturer’s documentation, these spectrometers typically have a FWHM of ~7% [45].

United states of America has the monitoring system called RadNet [46]. RadNet also employs gamma spectrometers with NaI(TI) crystals which are size of 2” x 2”. Based on data acquired on May 28th, 2020, there were 142 detectors which report gamma radiation levels, yet there is no data how many of them have scintillation detectors, but most of the models that are used, are based on such.

Another usage of gamma spectrometers is in border control, where the mandatory check-ups are held to assure that any illegal or dangerous items are being brought into the country. Example of such device is “identiFINDER® R400” produced by “Teledyne FLIR LLC”. This spectrometer is the most widely deployed handheld radionuclide identification device (RID) in the world. It is used to detect, locate, measure, and identify radioactive sources and produces rapid visible, audible, and tactile alerts that expedite response measures. It is also based on scintillating crystals, yet it have few variants with different material that crystal is made of, e.g. NaI(Tl), Nal shielded with tungsten or LaBr3. Typical FWHM for NaI based crystals is the same of about 7%, where manufacturer shows that detectors with LaBr3 have a resolution of ~4.5% [47].

Based on such popularity of gamma spectrometers in simple background radiation measurements and unknown radiating material identification, there is no doubt that such devices are in need for casual use as well. The biggest problem with commercial detectors is its price, which means that creating an open source gamma spectrometer based on obsolete dosimeters will be beneficial for anyone interested in gamma spectrometry.

2. Materials, Instruments and Methods

To construct gamma spectrometer based on scintillation detector, all the before mentioned parts are needed: scintillating crystal, PMT, voltage divider, pulse processing circuit with MCA, and high voltage power supply.

2.1. Barebones

One of the criteria of making an open source spectrometer is wide availability and low cost, but still being reliable, the best way is to take already existing device and see how it can be improved. So happens that the russian СРП - 88Н dosimeter is the perfect fit for this case.

Fig. 20. СРП-88Н dosimeter

This device has a 2.5 x 4 cm NaI(Tl) scintillating crystal, ф3у – 85 PMT that has 11 dynodes, voltage divider, high voltage power supply, great housing with additional shielding, and pulse processing circuit. The main problem with this dosimeter is that it is working as pulse counting device, rather than a spectrometer. It has all the required parts to work as a spectrometer, only the pulse processing circuit needs to be upgraded.

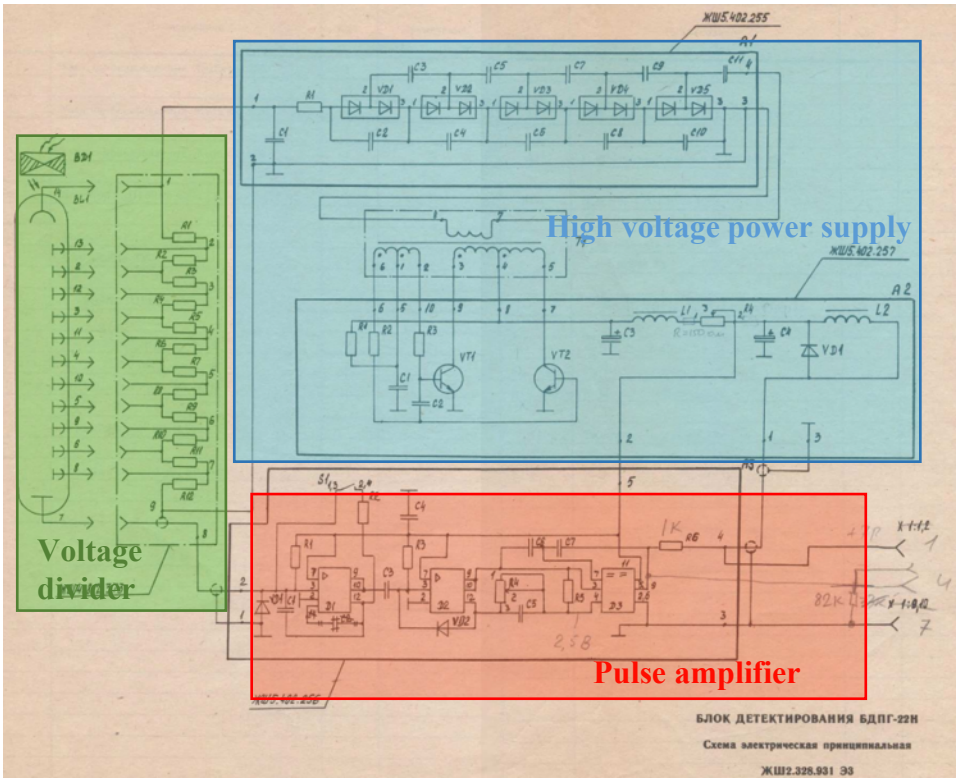

Fig. 21. СРП-88Н dosimeter electronic circuit scheme [48]

At first, the unprocessed output pulse of the detector was checked with an GDS-1022 oscilloscope. As can be seen in the figure 22, pulses are present, but there is a lot of noise as well, which comes from the built in HVPS.

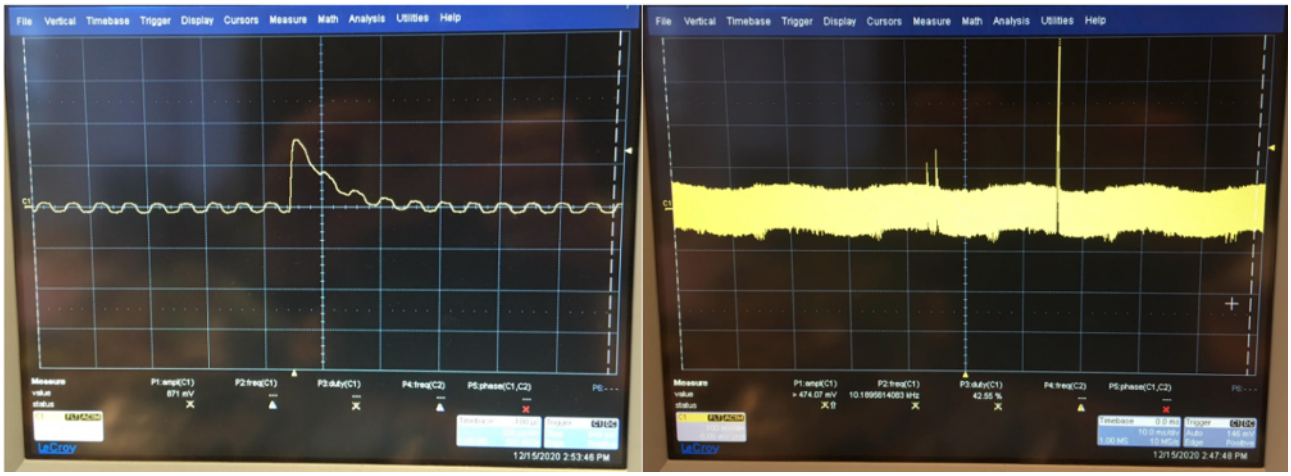

Fig. 22. Output result of originally set up PMT tube.

Such noise level and pulse shape are not very suitable for further processing. This means that now there are two missing puzzle pieces to have a fully functional scintillation detector: HVPS and pulse processing circuit.

2.2. Complete set

2.2.1. Scintillating crystal

It is a must to check scintillating crystal quality that it does not have any cracks or other visible defects such as yellow stains, which show that it was exposed to humid environment. Any defect in the crystal can have an effect on the output pulse because it blocks already produced light photons to pass through the crystal.

2.2.2. PMT

When looking at PMT visually, it is necessary to check there is still a vacuum inside it. First giveaway of vacuum absence is the photocathode color. For фэу – 85 it should have a color as shown in figure 23(*b*). Also, it should not have any defects, like bent pins, which could lead to having difficulties hooking it up to a voltage divider.

Fig. 23. Broken photocathode of the PMT (*a*) and unbroken (*b*)

2.2.3. Voltage divider

According to the manufacturer's technical datasheet, recommended фзу – 85 PMT circuit for voltage divider can be seen in the figure below.

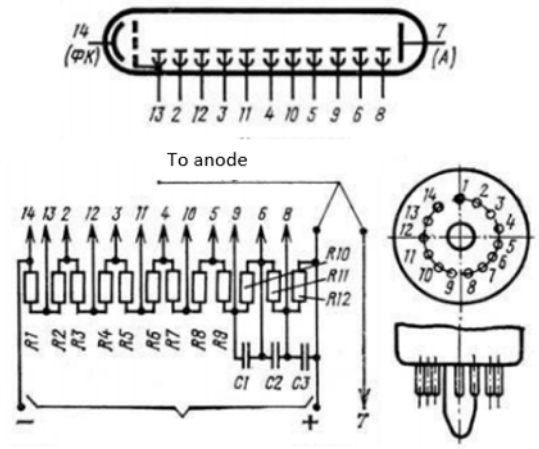

Fig. 24. Recommended voltage divider circuitry to power фзу – 85.

Spec sheet recommends using tapered voltage divider, with capacitors connected in series to resistors between the four last dynodes. Values for resistors are given at a coefficient of R, where R1-R2 must have 2R resistance, R3-R10 – must have R resistance and R11-R12 must have 1.5R of resistance. Recommended resistor value to use is 1 MΩ. For capacitors – less or equal to 0.05μF [49]. As known from literature review, capacitors are added to increase the linearity, since they can provide the current if voltage drops between the last dynodes, which in this case turned out to be not necessary. Tapered voltage divider employs higher resistor values near the photocathode to improve signal-to-noise ratio, and higher values near the anode to minimize space charge effects.

Considering the manufacturer's recommendation, new voltage divider was made with the correct resistors' values, because original implementation did not follow the guidance. Newly made voltage divider can be seen in figure 25. Main aim is to have the voltage divider as close to PMT as possible, to avoid any induction in the circuit to not interfere with the photocurrent.

Fig. 25. New voltage divider circuitry for фзу – 85

This simple implementation of voltage divider showed acceptable results. However, to improve it, printed circuit board could be designed and printed, so whole circuitry is closer to PMT and would not contain long wires to the resistors, because surface mount device components could be used. This would help to avoid even more electronic noise.
It is worth noting that in СРП - 88Н originally the PMT is connected to high negative voltage, where in datasheet and this case, high positive voltage is used. Positive voltage allows to connect cathode to ground, which minimizes noise caused by surrounding electric potential.

2.2.4. High voltage power supply and signal processing hardware

After analysis of various products, a device called GS-USB-PRO made by “Gammaspectacular” was chosen (figure 26). According to its technical documentation, it is a “Plug’n’Play” solution, which was confirmed to be not true due to manufacturers error and faulty rail-to-rail amplifier (LM6142). Not considering that, GS-USB-PRO is very easy to operate, it uses 5V as main input, and is capable to output up to 2000V. Also, it has an USB and 3,5mm audio jack outputs which allows multiplatform use.

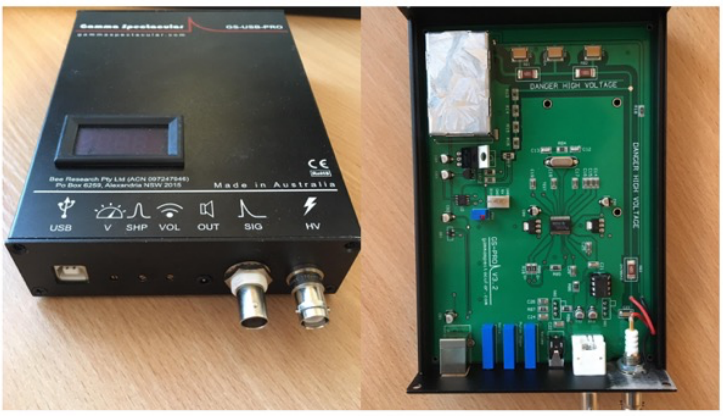

Fig. 26. GS-USB-PRO by “Gammaspectacular”.

From signal processing point of view, this device has everything what is needed for the analog signal to be converted to digital value. To be more exact: rail-to-rail amplifier, low/high-pass filters and analog to digital converter which has 16 bits.
Most of operating systems are able to recognize this device as an external sound card, meaning it is easy to perform gamma spectrometry with any available open-source multichannel analyzer software. Since GS-USB-PRO is selected, all the previously existed circuitry inside the СРП - 88H can be taken out.

2.3. Signal processing software

To analyze the already processed signal from GS-USB-PRO „PRA“ software package was chosen. It has a simple user interface with all the needed functionalities.

2.3.1. Input device

The very first step that has to be done once „PRA“ is opened is the audio interface selection. When GS-USB-PRO is plugged in it is recognized as an external sound device called “USB AUDIO CODEC”. In the dialog box (figure 27) it is necessary to select it as input device, as well as sampling rate as 384000 and 16 Bits. Output device has no relevance in spectrum result.

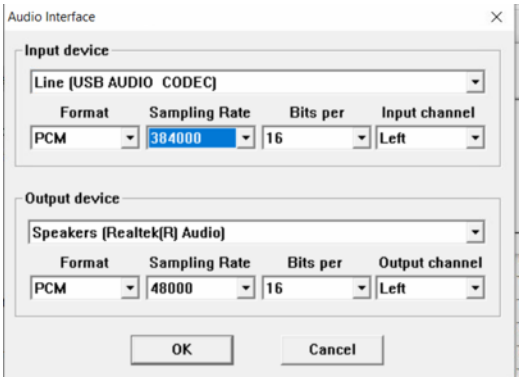

Fig. 27. Audio interface selection in “PRA” software

Once this is done, some parameters must be updated in the “Data Acquisition and Analysis” dialog box.

2.3.2. Data acquisition parameters

These are the main parameters that have to be adjusted for better resolution or clearer result:

Data acquisition parameters:
“Min height/arb.u” parameter means what is the amplitude that is acceptable in the measurement, the lower this value is, the more low amplitude noise can intervene the spectrum, yet if it’s too high, low energy photopeaks will be chopped off.
“Boost gain” if the pulse amplitude is too low, this parameter allows to boost it.
“Use shape method” is a necessary tool to enable. “PRA” has an ability to check incoming pulse shape and filter out if it does not correspond to the acquired one (pulse shape acquisition will be covered later). This helps to filter out noise, pulse pileups or afterpulses.
“Max distortion/arb.u” is the tolerance/percentage of the pulse. Anything that is outside of the tolerance, will be filtered out and not included in the spectrum.

Pulse heigh histogram parameters:

"Bin size" is the equivalent of number of channels. This is done to combine actual channels into larger units, because with sound cards there are 64 000 channels, which is way more than needed for spectrometry. This arbitrarily sets sound card original channels to value from negative 100 to positive 100, so when it's 0.1, there are 1000 channel division in a range from 0 to 100 arbitrary units. *"Use calibration"* tick box is used when there are some calibration points already set, so it changes abscissa axis to correspond to the values set in calibration dialog box.

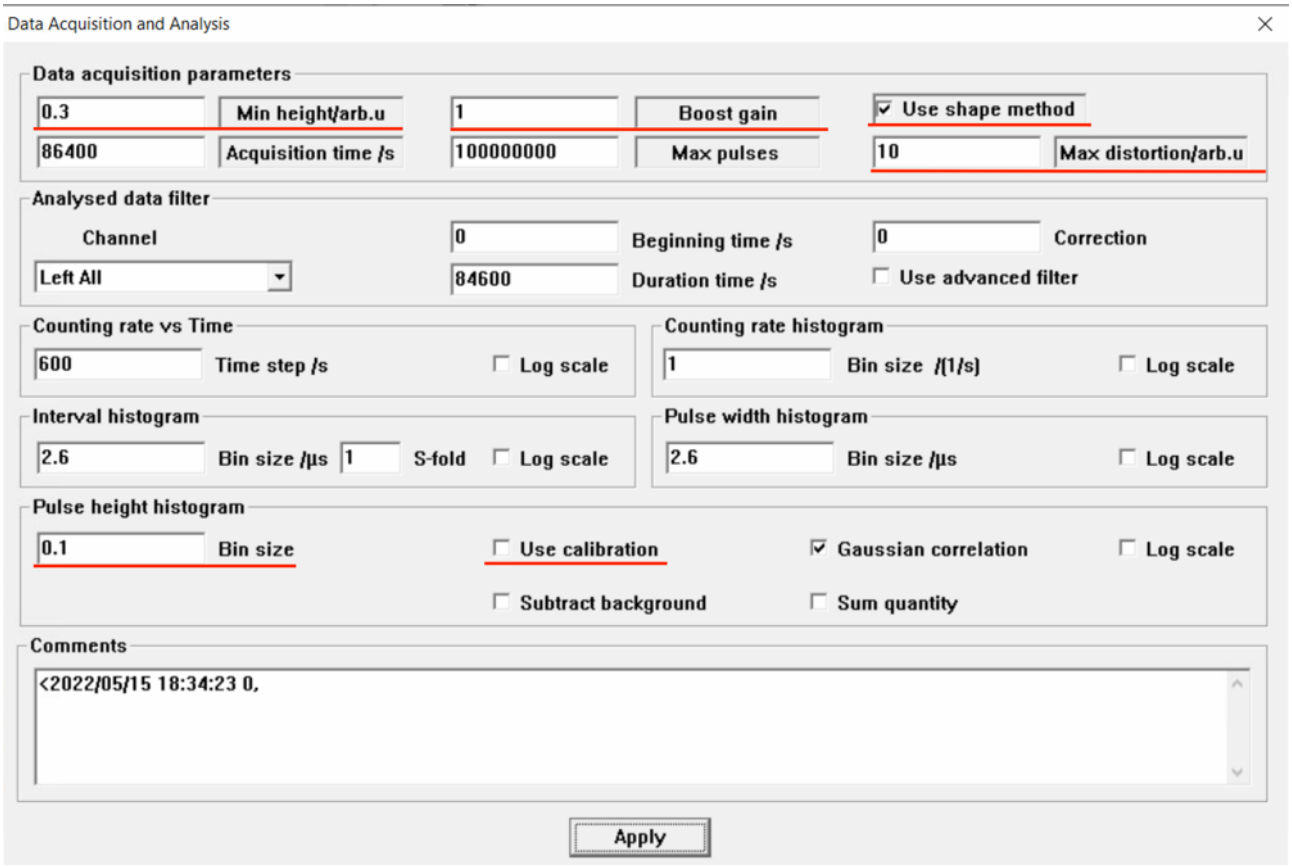

Fig. 28. Interface of data acquisition parameters window of "PRA" software

For the constructed detector the parameter values were selected which can be seen in figure 27 and 28.

2.3.3. Pulse shape

The signal that comes from GS-USB-PRO sometimes can be distorted or contain noise, but it is known that the pure signal from PMT is a simple pulse. Meaning, no small or short pulses before and after the actual pulse should occur. To filter out any bad shape pulses like the ones with afterpulses or pulse pile ups, pulse shape is acquired. "PRA" software allows to describe an ideal pulse and compare every incoming one with the one that is set. If incoming pulse does not match the shape, including the allowed distortion mentioned above, it won't include that pulse in the results.

The first thing once everything else is set up, is to press "Start Pulse Shape Acquisition" and wait to collect about 10000 – 15000 pulses. "PRA" software will measure every pulse from collected ones and will average and "normalize" it to make a standard pulse shape representation.

Once this step is done, dialog box pops up with values which describes the "correct" pulse shape (figure 29).

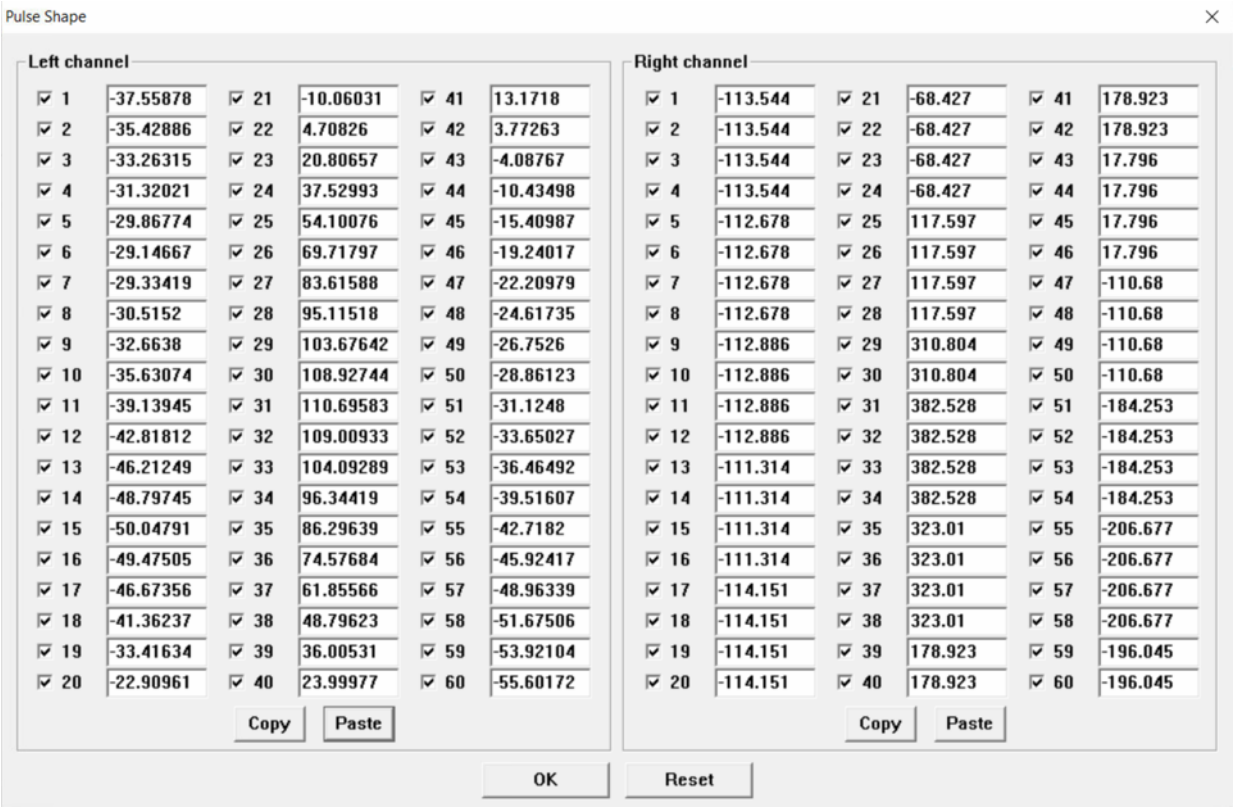

Fig. 29. Pulse shape described in "PRA" software

Right channel can be ignored, since in the input device section input was selected from left channel. These numbers can be plotted, and it will show how the actual pulse looks like, this can be seen in the figure 30.

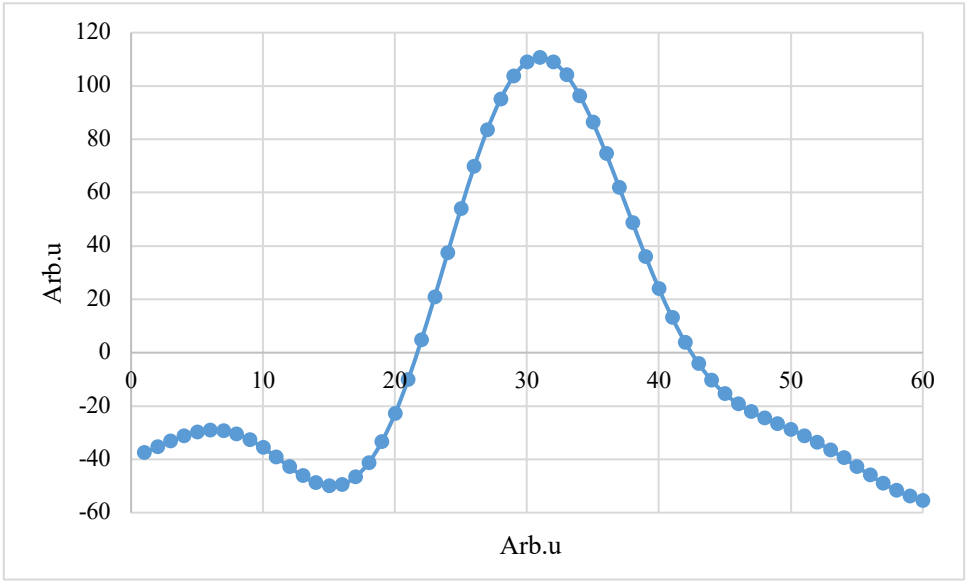

Fig. 30. Pulse shape calculated in "PRA" software

This pulse is normalized, which means that linear function is applied to the pulse shape which makes the result of the dot product to independent of any constant shift of the baseline.

2.3.4. Calibration

To get more information of the peaks, calibration must be done. Since analog-to-digital conversion just assigns any analog pulse height to the appropriate digital value, there is no way to know what height corresponds to what energy of the gamma photon before doing calibration. It takes few steps:

1. Radioactive source of known material, in this case ^{137}Cs is be placed near the detector and recorded for at least 10 – 15 minutes to have a clear peak.
2. Highest peak in the spectrum is correlated to the energy peak of known radioactive source, in this example – ^{137}Cs, with most common decay product energy of 661.59 keV.
3. When highest peak is found whole spectrum (or scale of graph) is shifted to make sure that the peak is on 661.59 keV energy level.

3rd step is achieved by clicking "Calibration" and entering the information from pulse height distribution into the table seen in figure 31.

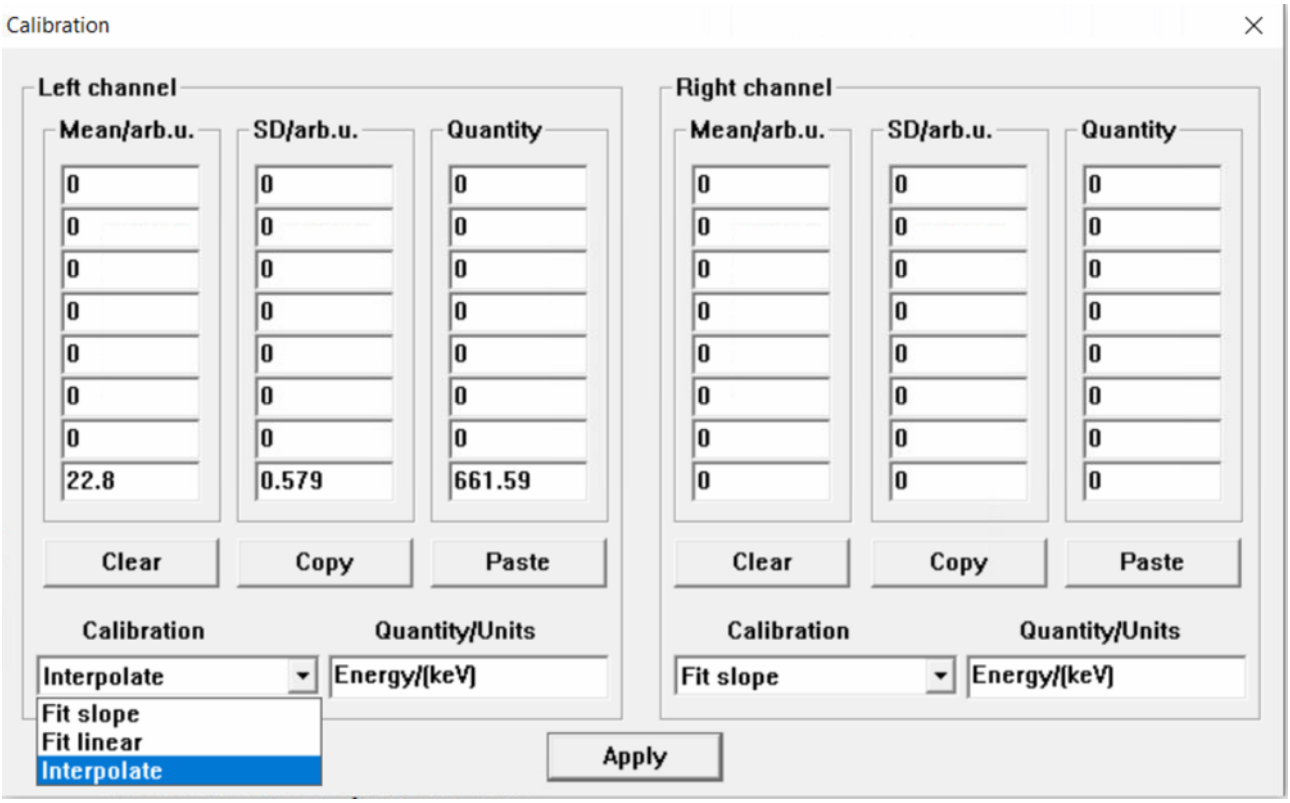

Fig. 31. Interface of calibration window in "PRA" software

In this example, ^{137}Cs photopeak has the highest count of pulses on the 22.8 arb. u., with the standard deviation of 0.579 arbitrary units.

It must be noted that there are three ways how energy is assigned to arbitrary unit, which can be seen on the left side of the figure 31: *fit slope*, *fit linear* and *interpolate*. If calibration includes only one energy, the best selection is either fit slope or linear, but if calibrating with more than one energy, interpolation must be chosen, because it will distribute the values across abscissa axis not in a linear way, but in the best way to correspond the actual values.

2.4. Reference data of spectrums

All the measurements of known radioactive sources were also made with commercially available handheld spectrometer “IdentiFINDER”. This device has a NaI crystal which is 35 mm x 51 mm size, or in other words, 56% bigger crystal than constructed device. Also, this handheld spectrometer comes with “winTMCA32” software package, which lets to analyze spectrums and automatically calculates energy resolution of selected peaks [47].

2.5. Final measurements setup

To easily perform measurements, operate the device and change samples old laboratory stand was employed, and together with some 3D printed parts GS-USB-PRO with the constructed detector probe was mounted to it. Also, 1 meter USB cable is used, which allows the device that runs “PRA” software, in this case laptop, to be placed nearby (figure 32).

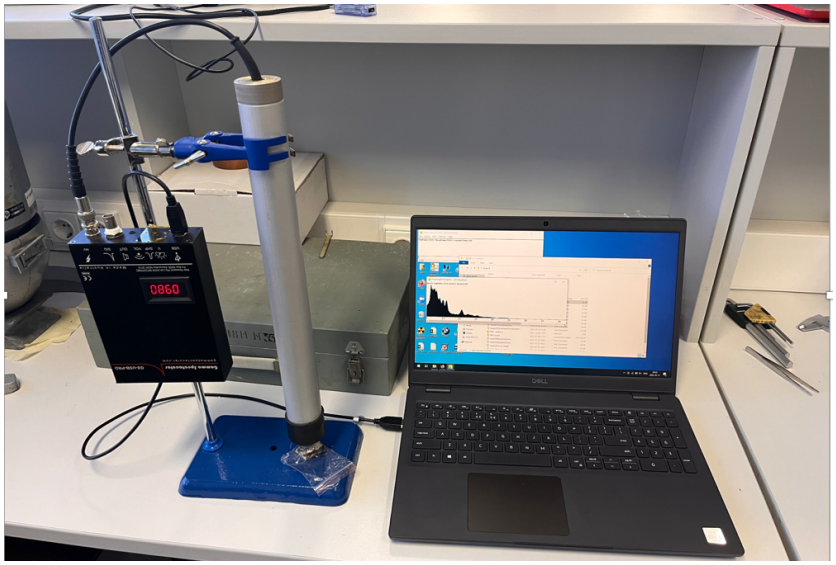

Fig. 32. Measurement setup

Some measurements were made in a lead shield, to avoid any unnecessary background noise. Also, the later mentioned radiating sources were placed at the bottom of the shield, which can be seen in figure 33.

Fig. 33. Lead shield and ionizing radiation source

3. Results

After the functional hardware was developed, a series of characterization tests were performed, to determine the performance of the equipment.

3.1. Determination of counts per minute plateau

As mentioned, PMT gain has a big dependency on the applied voltage, meaning there is a relation between applied voltage and the digital value, i.e., channel that photopeak is assigned to. This connection has an effect on one of the main gamma spectrometer characteristics – energy resolution. Since pulse shape and other parameters are already selected, determination of counts per minute (CPM) plateau includes measuring two ^{137}Cs sources with detector placed inside the lead shield for 5 minutes, raising applied voltage by the step of 25V, starting from 500V up to 1000V. Then from measurement of 5 minutes, average counts per minute was calculated. The aim is to see at which voltage counting rate per minute settles (figure 34). Stable CPM is important to minimize uncertainty when changing samples or other detector parameters.

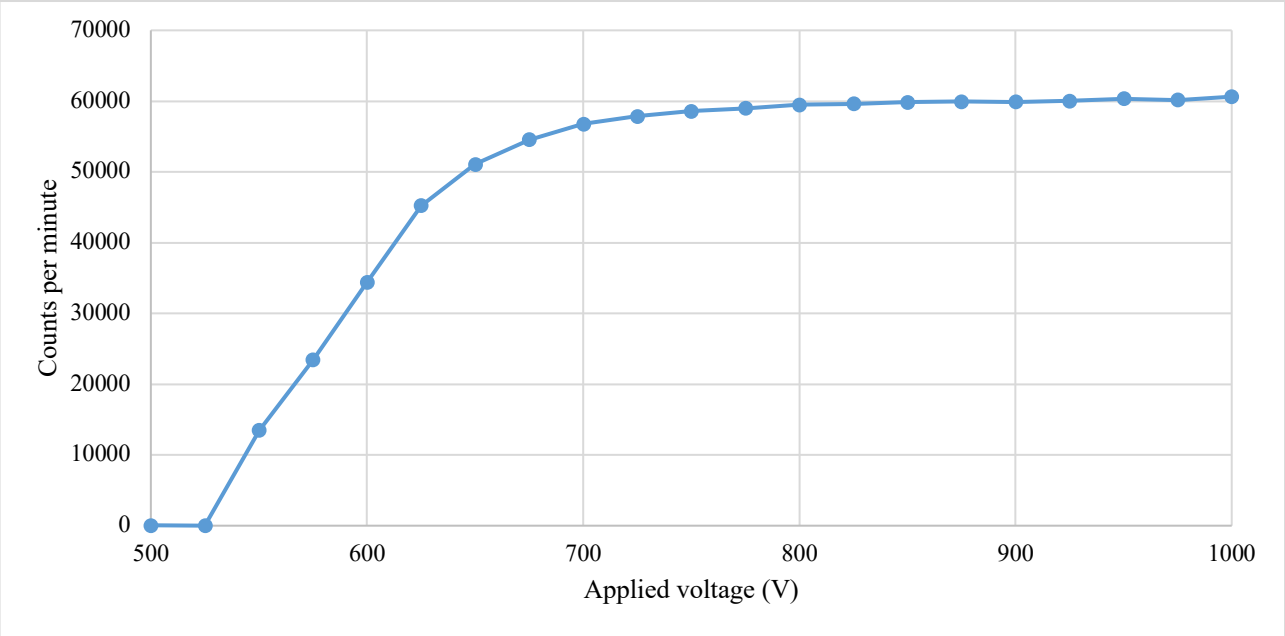

Fig. 34. CPM dependency on applied voltage between 500V and 1000V

As can be seen from figure above, counts per minute stabilizes at around 800 Volts. Yet if zoomed in (figure 35) at the range between 800V and 1000V, plateau seems to be somewhere around 850V and 900V.

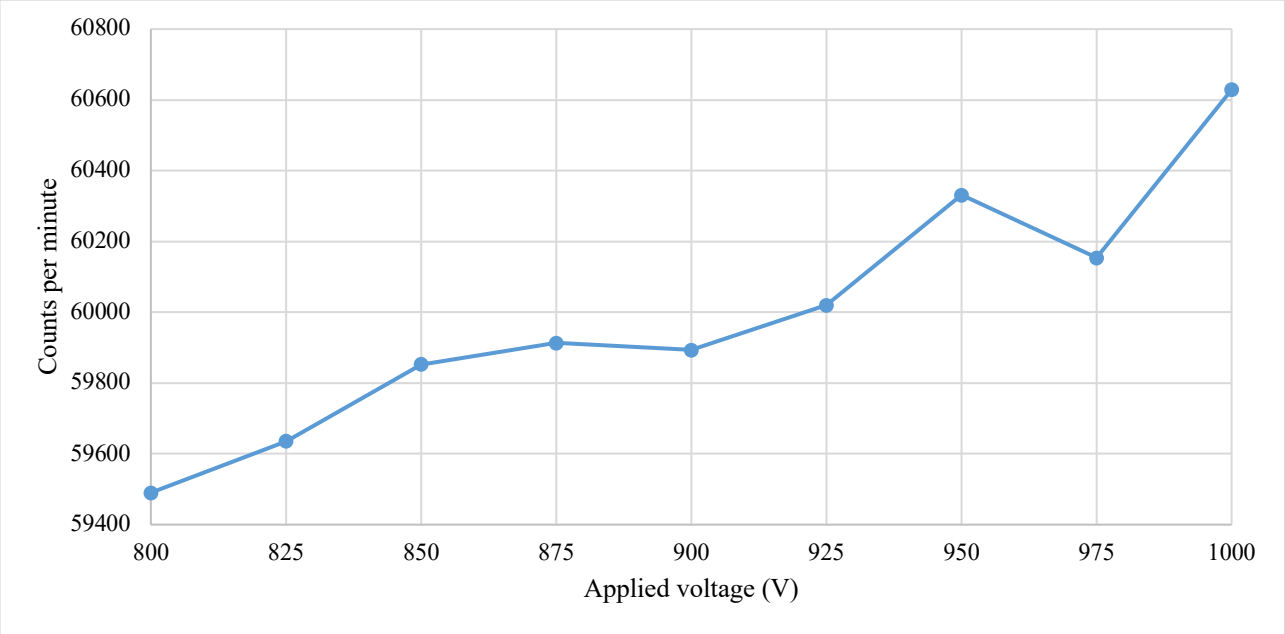

Fig. 35. CPM dependency on applied voltage between 800V and 1000V

To make sure, additional measurement was taken, also for 5 minutes each inside the lead shield with two ^{137}Cs sources, just the voltage step was lowered to 10V. Results can be seen in figure 36.

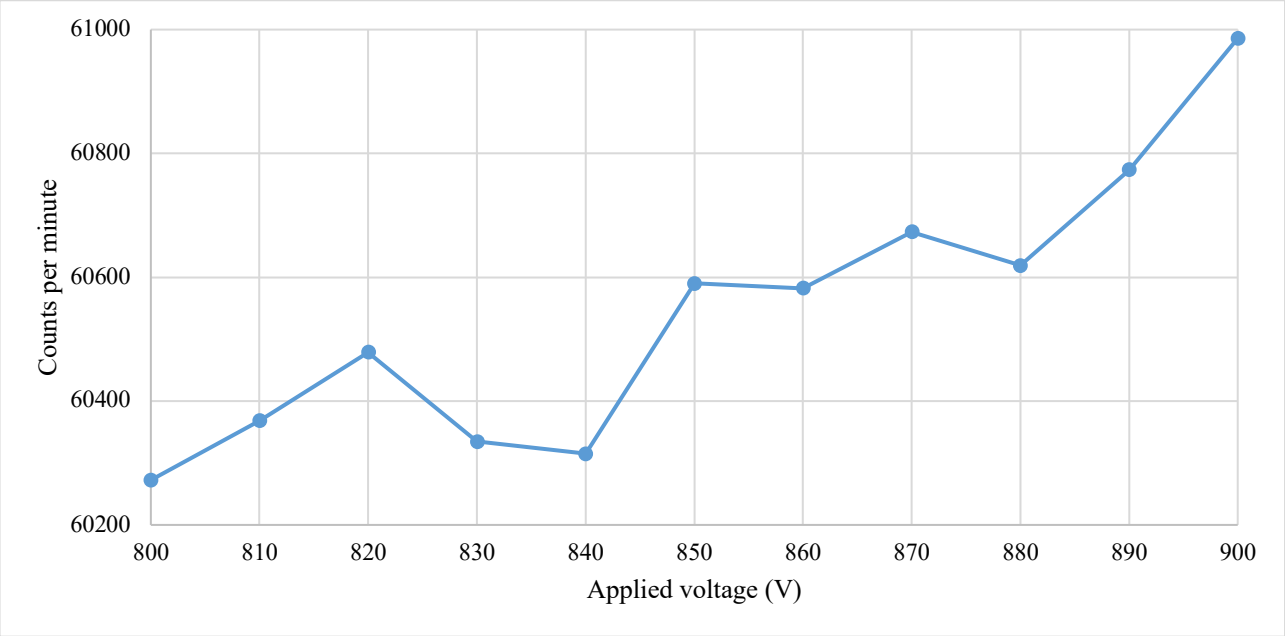

Fig. 36. CPM dependency on applied voltage between 800V and 900V

It is quite clear that the working voltage should be selected between 850V and 860V if looking only at CPM. Highest deviation in 5 measurements for each voltage is for 890V, which is 0.77%, and lowest for 840V – 0.04%.

Meanwhile, it can be seen that CPM are higher in second round of measurements for the same voltage than in previous one for around 2.3% on each voltage. This could have happened because position of ionizing radiation sources or the detector has changed between the measurements, or because of instability of the detector since it has to warm up a little bit. This will be discussed later.

3.2. Determination of energy resolution

Energy resolution was determined for different voltage as well. The measurement was the same, 5 minutes for each voltage between 800V and 900V with two ^{137}Cs sources and step of 10V. Due to working principle of PMT, which was mentioned above, the higher the voltage, the higher the channel number same energy gamma ray photon will be assigned to. Even though CPM plateau was found between 850V and 860V, it must be checked that pulses height distribution is also acceptable. Nonetheless, it can be fixed in software, for example shrinking the spectrum a bit with merging few channel numbers to represent one voltage value.

Values up to an 800V does not make much sense to measure and show, because the spectrum is very squeezed, due to low number of photoelectrons, meaning, it is not multiplied enough, so amplitude could not be differentiated to be assigned to different digital values. As well as above 900V, due to too high photon count, which produces afterpulses.

As can be seen in figure 37, the higher the applied voltage the more stretched spectrum is and vice versa. The aim is to find a sweet spot at what voltage spectrum has the lowest energy resolution.

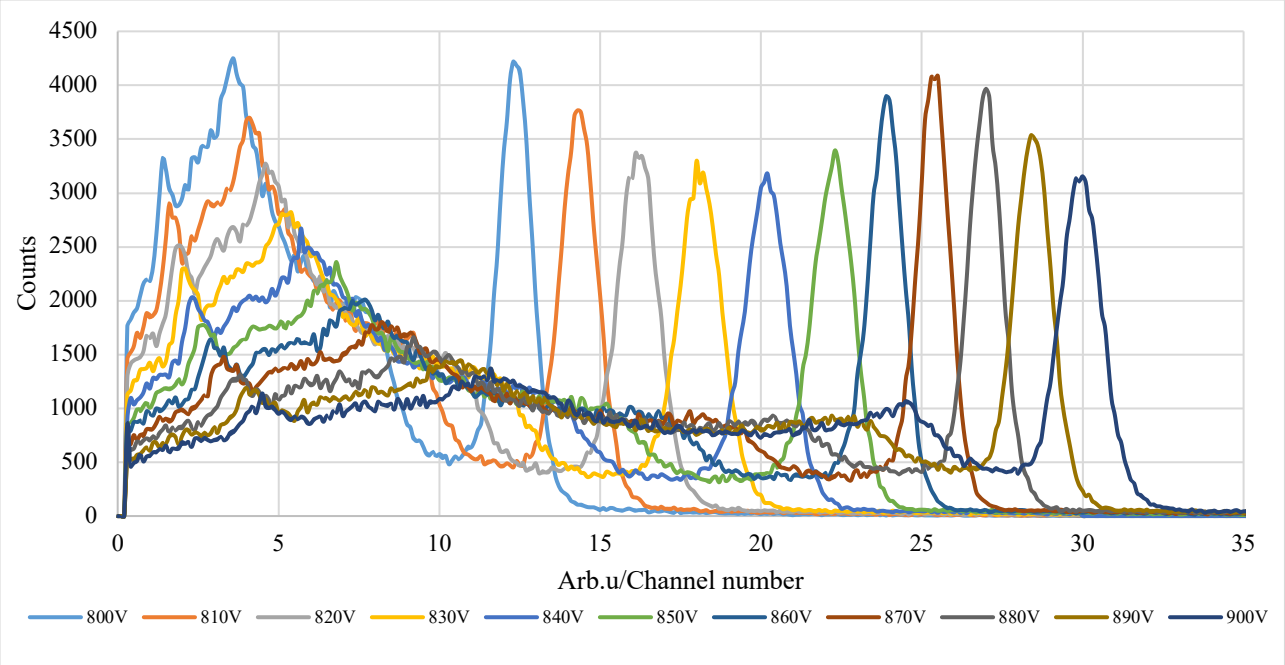

Fig. 37. Energy resolution dependency on applied voltage between 800V and 900V

Energy resolution was calculated using equation 3. As can be seen from table 2, lowest energy resolution turned out to be when applied voltage is 860V. Which is the same voltage if looking at CPM stability, meaning 860V is the optimal value to operate the detector that was made.

Table 2. Energy resolution dependency on applied voltage between 800V and 900V

Applied voltage, V	**Energy resolution of ^{137}Cs, %**
800	10.57
810	10.49
820	9.94
830	8.89
840	8.42
850	6.73
860	**5.02**
870	5.10
880	5.19
890	5.28
900	5.67

3.3. Determination of stability

While analyzing literature it was noted that there are short-term and long-term drifts. To check how this detector drifts it was measured for 24 hours, again with two ^{137}Cs sources and the voltage of 860V, because this was determined to be the most suitable one.

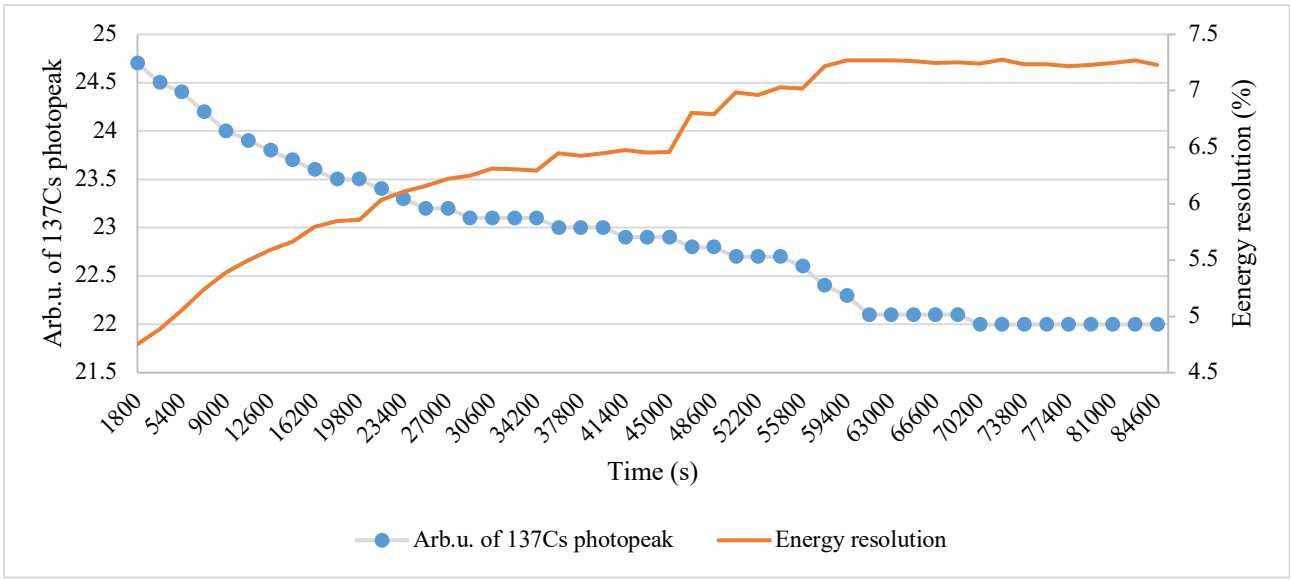

Fig. 38. Energy resolution and ^{137}Cs photopeak dependency on operating time

From figure 38 it can be seen that the longer detector is turned on, the more ^{137}Cs photopeak is pushed to the right side of the spectrum, started at 24.7 arb.u and end up at 22 arb.u. Also, the resolution worsens over time as well. Only after 19.5 hours both photopeak and resolution stabilizes. Knowing that, to make a repeatable measurement with this detector, it should be left turned on for 20 hours before measuring.

3.4. Spectrums of known sources

To check the validity of calibration of the developed instrument, spectrums of known sources are acquired and compared with the commercially available device – ”IdentiFINDER” made by “Target”. Spectrums of known sources were measured for 10 minutes. DiY spectrometer was powered on for 24 hours prior measurements.
To easier reference spectrometer that is made in this work, it will be called GS-JBUBG-85.

3.4.1. Manipulation of acquired known sources data

In the measurement of determination of energy resolution by varying applied voltage, energy resolution values are calculated by hand using equation 3. The conclusive values of bounds of the peak to calculate FWHM are selected based on visual observation. However, “IdentiFINDER” has a software named “winTMCA32” which is made for analyzing spectrums acquired by the device. It has a feature to find peaks in the spectrum. With a little bit of changing original “IdentiFINDER” spectrum files, it is possible to upload GS-JBUBG-85 spectrum to the “winTMCA32” software. This approach is used in later energy resolution determination because it is more accurate, since the same energy steps are used.
Since radioactive materials spectrum measurements were made with two different detectors it was observed that the sensitivity of the detectors is not the same, which means that the very first step that has to be done is to normalize counts per channel so it can be compared and visualized in one graph. This is achieved by taking the highest count value of selected element photopeak of “IdentiFINDER” and dividing that value by the highest count value of selected element photopeak of constructed detector. Such calculation yields a ratio of a difference between counts. Then all the counts of whole spectrum which were acquired with assembled detector are multiplied by the ratio. Channel width is practically identical in both detectors, although it can be changed in software, nothing had to be done to align it.
Spectrums of known sources were acquired without shielding from background radiation, but background counts are subtracted from the final counts.

3.4.2. Spectrum of ^{137}Cs

The spectrum of ^{137}Cs can be seen in the figure 39. Normalization ratio was calculated from the only photopeak, and ratio value is 3.58. Both spectrums show clear ^{137}Cs photopeak. According to "winTMCA32", "IdentiFINDER" has an 8.2% energy resolution, where GS-JBUBG-85 has 7.3%. Compton edge is also visible, as well as backscatter peak, because both detectors have high density material, aluminum, around scintillating crystal.

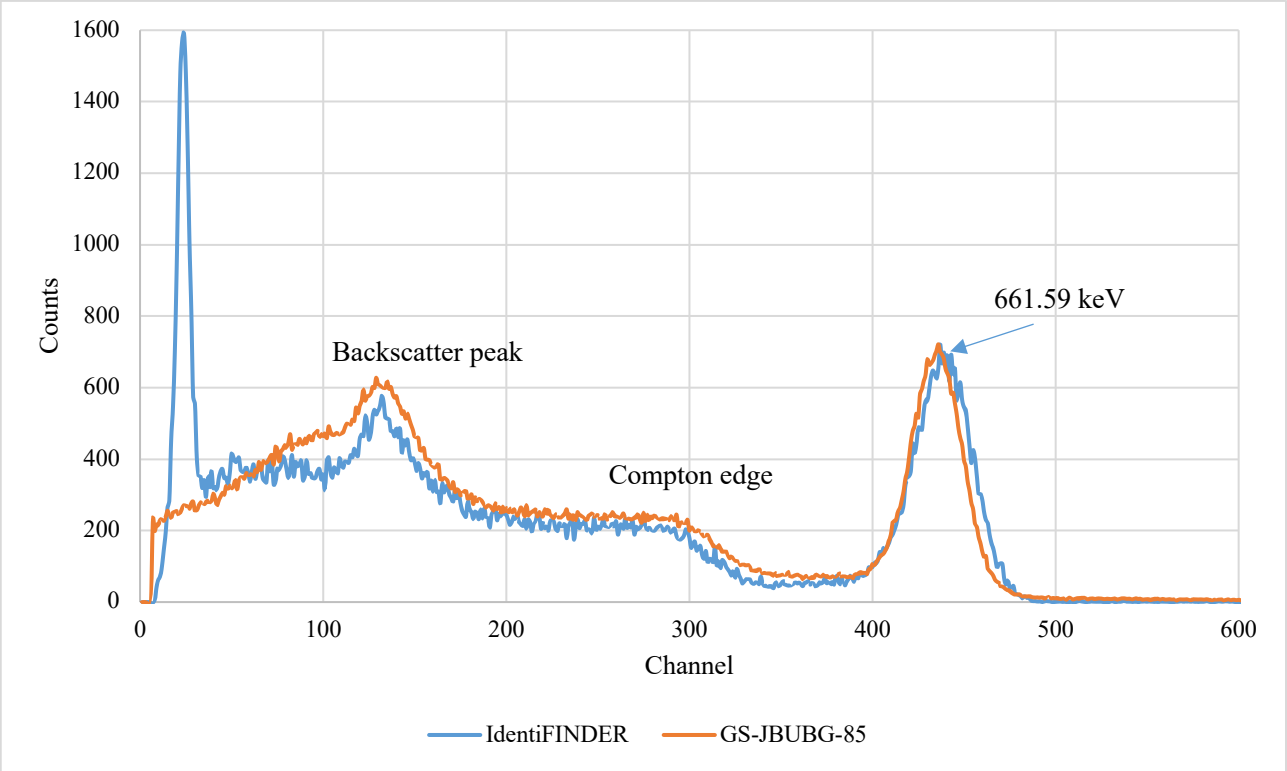

Fig. 39. Spectrum of ^{137}Cs

One thing that is missing in the constructed detector spectrum is Barium X-ray peak which should be ~32 keV when calibrated, but in this case, on the very left side. Barium X-ray peak nature is internal conversion when gamma ray does not exit the atom and ejects K shell electron, and its place is filled with electron from L or M shell. This is probably because GS-JBUBG-85 does not contain any Barium compounds or majority of very low energy photopeaks are removed in software, because it does not differ much from low amplitude noise. No other peaks are analyzed because ^{137}Cs is monoenergetic gamma emitter.

3.4.3. Spectrum of ^{133}Ba

In the spectrum of ^{133}Ba it is the same situation with very low energy Barium X-ray peak (figure 40). The graph ordinate axis is formatted in a way that ^{133}Ba X-ray peak is ignored, so it is possible to compare other energy peaks a bit better. The normalization ratio was calculated from the second highest peak and the ratio value is 4.02.

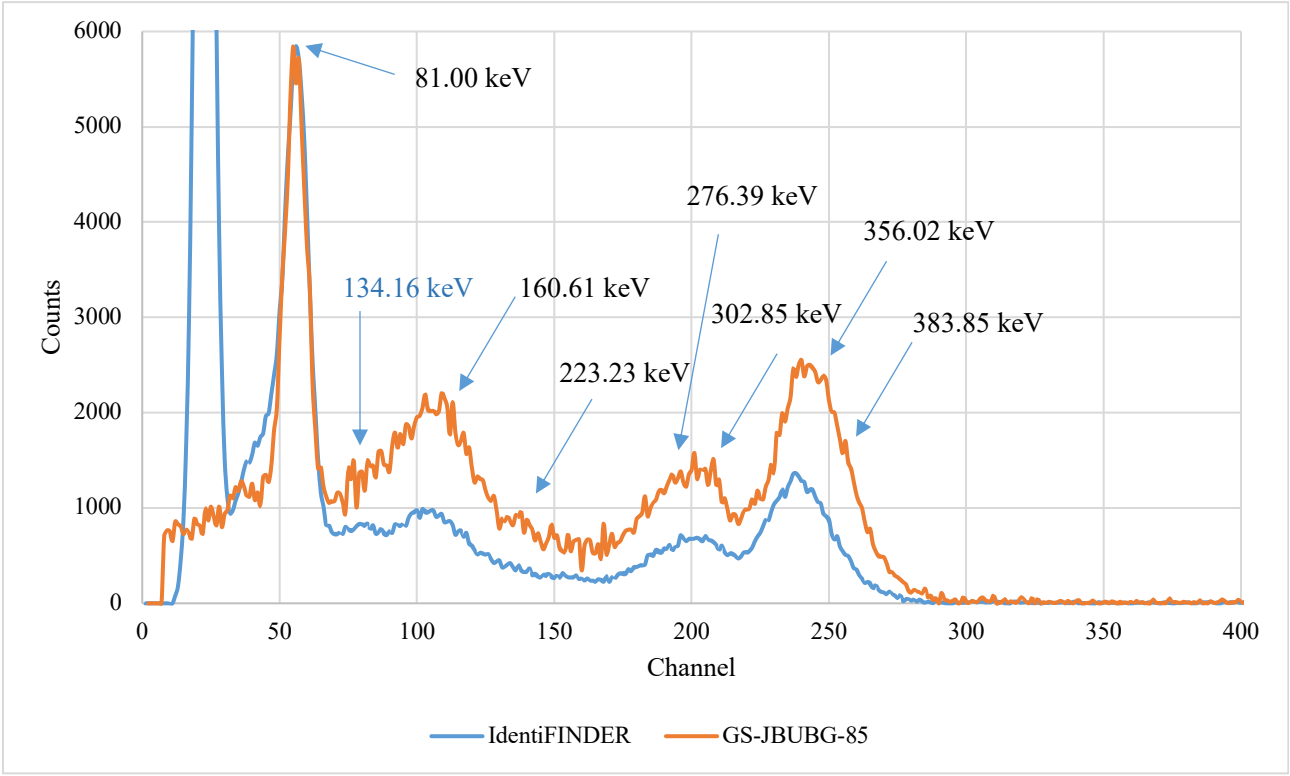

Fig. 40. Spectrum of ^{133}Ba

The very first obvious peak from right to left is typical for ^{133}Ba and it has energy of 356.02 keV. Energy resolution for GS-JBUBG-85 yielded 11.8% and 11.7% for "IdentiFINDER". Second from the right is 302.85 keV peak formed of 80 keV energy photons (third peak from right to left) plus the 223.23 keV energy photons. Another peak which is a bit visible in "IdentiFINDER" spectrum where it is not so obvious in GS-JBUBG-85 is around 134.16 keV which is formed combining energies from 81.00 keV photons and 53.16 keV gamma ray photons emitted from ^{133}Ba [50,51].

Table 3. Gamma energies of ^{133}Ba and visibility of it in acquired spectrum [50,51].

Gamma energies of ^{133}Ba (keV)	**Intensity (%) ± uncertainty (%)**	**Visible in acquired spectrum**	
		"IdentiFINDER"	**GS-JBUBG-85**
81.00	34.06 ± 27	Yes (res. 18.6%)	Yes (res. 16.7%)
160.61	0.64 ± 8	Yes (res. 21.9%)	Yes (res. 27.3%)
223.25	0.45 ± 4	Yes	Yes
276.40	7.16 ± 22	Yes	Yes
302.85	18.33 ± 6	Yes (res. 15%)	Yes (res. 13.9%)
356.02	62.05 ± 19	Yes (res. 11.7%)	Yes (res. 11.8%)
383.85	8.94 ± 3	Yes	Yes

As can be seen from table 3, if comparing 356.01 keV energy resolution to other ones, it is at least few percent lower and probably other peak resolutions are not worth measuring, because these points will not be used in calibration.

3.4.4. Spectrum of ^{228}Th

In the spectrum of ^{228}Th that was acquired with Identifinder, again high count of impulses were recorder of the very low energy photons. Same as in ^{133}Ba spectrum, ordinate axis on figure 41 is changed to show maximum value of 8000 counts. For ^{228}Th spectrum the normalization ratio was calculated from the second highest peak, ratio value is 2.

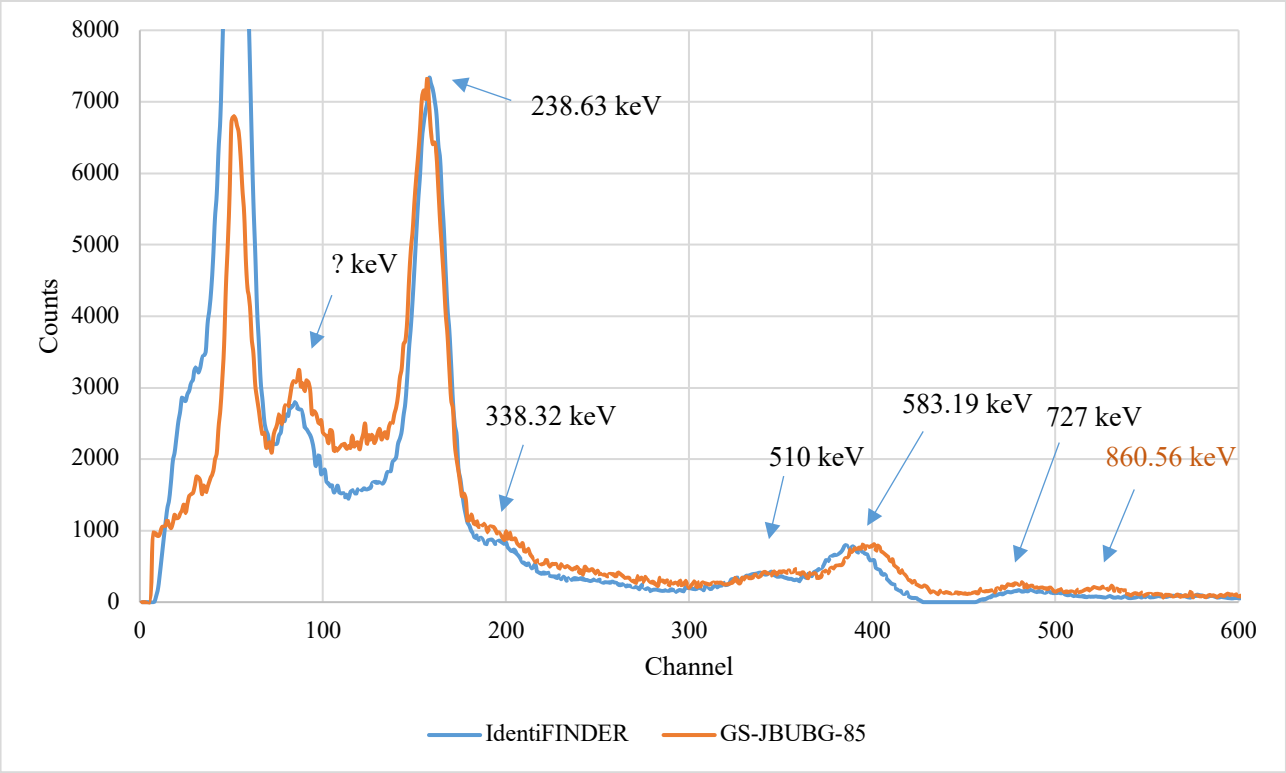

Fig. 41. Spectrum of ^{228}Th

Spectrum of ^{228}Th shows typical peaks for such element. The highest one is located at 238.63 keV and "IdentiFINDER" has energy resolution of 11.9% for this peak, where GS-JBUBG-85 has 12.5%. It is not worth measuring other peaks resolution, because, as mentioned, wide peaks are not suitable to be a calibration point.

Table 4. Gamma energies of ^{228}Th and visibility of it in acquired spectrum [52,53,54].

Gamma energies of ^{228}Th (keV)	**Visible in acquired spectrum**	
	"IdentiFINDER"	**GS-JBUBG-85**
238.63	Yes (res 11.9%)	Yes (res 12.5%)
338.32	Yes	Yes
510	Yes	Yes
583.19	Yes	Yes
727	Yes	Yes
860.56	No	Yes

3.4.5. Spectrum of ^{152}Eu

^{152}Eu spectrum can be seen in figure 42. Second highest peak was selected for normalization ratio and the ratio value is 2.35. Ordinate axis is formatted so extra low energy peak from "IdentiFINDER" is again ignored.

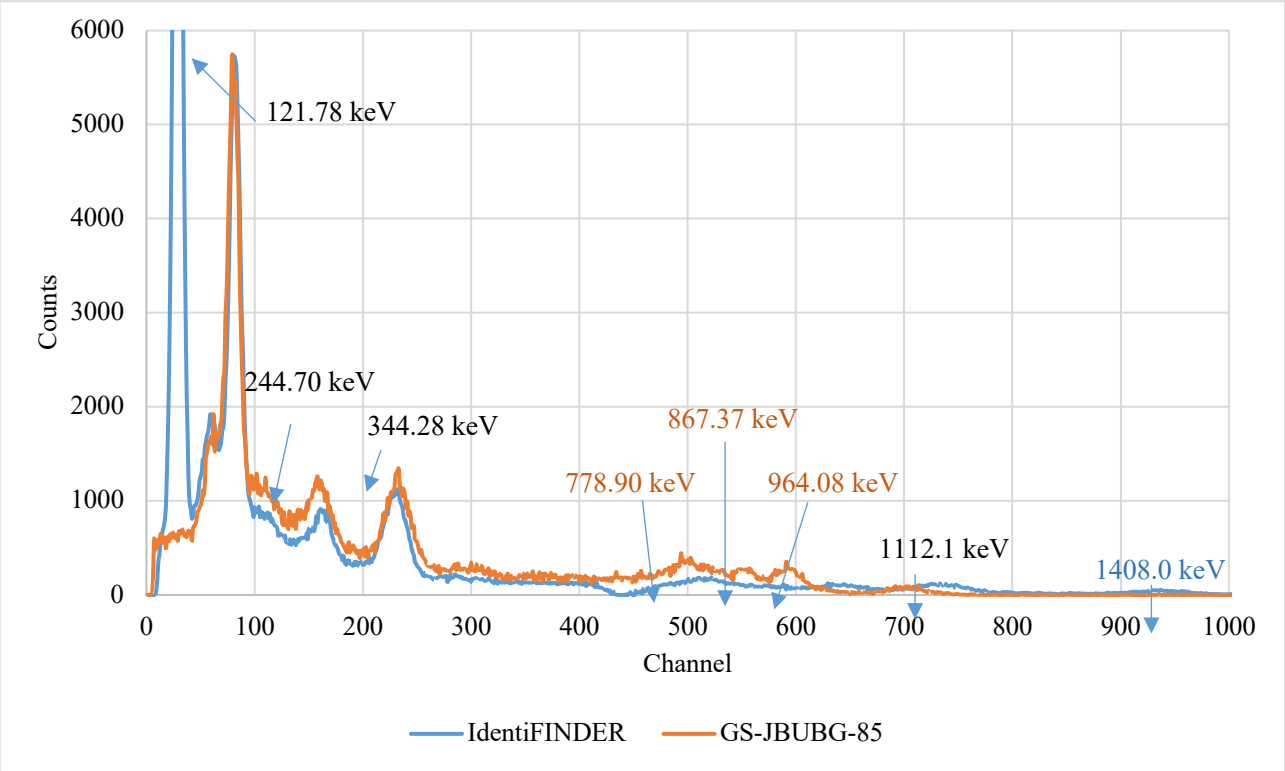

Fig. 42. Spectrum of ^{152}Eu

Energy resolution of highest peak of 121.78 keV for "IdentiFINDER" is 14.2% and for GS-JBUBG-PRO is 14.9%. Other peaks of 244.70 keV and 344.28 keV are clearly visible in both detector spectrums, but going to the higher energies, up to 1 MeV, constructed detector shows higher efficiency. However, looking even further, it is noticeable that GS-JBUBG-85 did not record any pulses of 1408 keV energies, where "IdentiFINDER" has a peak. This behavior can be explained, because "IdentiFINDER" has a bigger scintillating crystal, where in GS-JBUBG-85 high energy photons are just passing through. Or due to software parameter, such as pulse shape tolerance level. High energy pulses have high amplitude, but if pulse shape is acquired using only background, as it is in this case, high amplitude pulses are filtered out.

Table 5. Gamma energies of ^{152}Eu and visibility of it in acquired spectrum [55]

Gamma energies of ^{152}Eu (keV)	**Intensity (%) ± uncertainty (%)**	**Visible in acquired spectrum**	
		"IdentiFINDER"	**GS-JBUBG-85**
121.78	28.58 ± 9	Yes (res. 14.2%)	Yes (res. 14.9%)
244.70	7.58 ± 30	Yes	Yes
344.28	26.5 ± 6	Yes	Yes
778.90	12.94 ± 15	No	Yes
946.08	14.6 ± 4	No	Yes

1112.1	13.64 ± 4	Yes	Yes
1408.0	21.00 ± 6	Yes	No

3.4.6. Spectrum of ^{226}Ra

^{226}Ra spectrum can be seen in figure 43. Peak of ^{214}Bi (609.31 keV) was selected for normalization ratio, and value is 2.8. Ordinate axis is formatted so extra low energy peak from "IdentiFINDER" is again ignored.

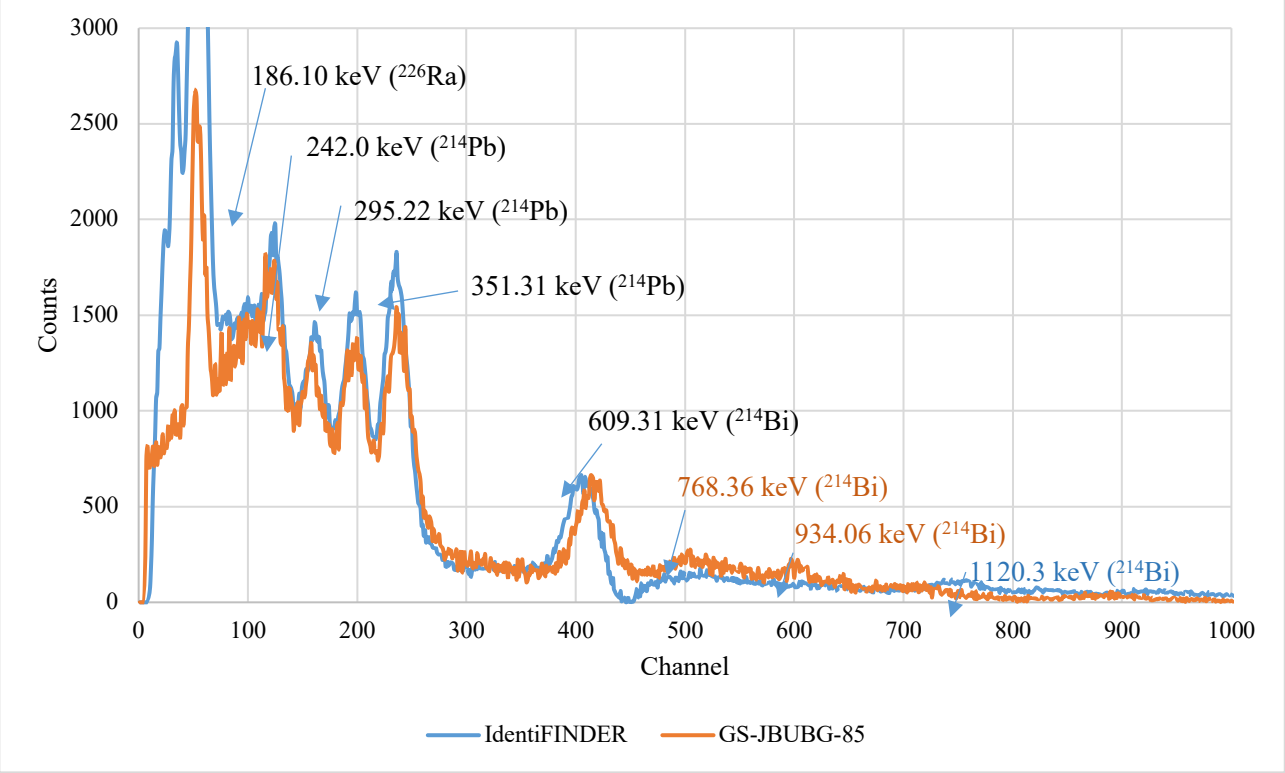

Fig. 43. Spectrum of ^{226}Ra

According to "winTMCA32" software, energy resolution of 609.31 keV peak for GS-JBUBG-85 is 7.9%, where for "IdentiFINDER" it is 8.1%. As mentioned in literature analysis, ^{226}Ra produces a few very clearly visible peaks and they are suitable for calibration/linearity determination. As observed in ^{152}Eu spectrum, "Identifinder" again does not show good response in energies between 600 keV and 1000 keV. However, peak at 1120.3 keV can be clearly seen, where GS-JBUBG-85 did not record impulses of such height.

Table 6. Gamma energies of ^{226}Ra and visibility of it in acquired spectrum [56]

Gamma energies of ^{226}Ra (keV)	**Intensity (%) ± uncertainty (%)**	**Visible in acquired spectrum**	
		"IdentiFINDER"	**GS-JBUBG-85**
186.10	3.51 ± 6	Yes	Yes
242.0	7.12 ± 11	Yes	Yes
295.22	18.15 ± 22	Yes	Yes
351.31	35.1 ± 4	Yes	Yes

609.31	44.6 ± 5	Yes (res. 8.1%)	Yes (res 7.9%)
768.36	4.76 ± 7	No	Yes
934.06	3.07 ± 4	No	Yes
1120.3	14.7 ± 2	Yes	No

3.5. Calibration curve

Nine points were selected to make a calibration curve for GS-JBUBG-85, it can be seen in table 7.

Table 7. Energies and arbitrary units that were selected for calibration

Element (energy (keV))	**Arbitrary unit in GS-JBUBG-85 spectrum**
^{133}Ba (81)	2.65
^{152}Eu (121.78)	3.9
^{228}Th (238.63)	7.8
^{152}Eu (344.28)	11.6
^{226}Ra (351.31)	11.75
^{133}Ba (356.02)	11.9
^{226}Ra (583.19)	19.7
^{226}Ra (609.31)	20.65
^{137}Cs (661.59)	21.75

As can be seen in the figure 44, GS-JBUBG-85 has a great linearity. Some energies could be added in an interval between 350 keV and 550 keV, but no radioactive materials were available which would radiate such energies.

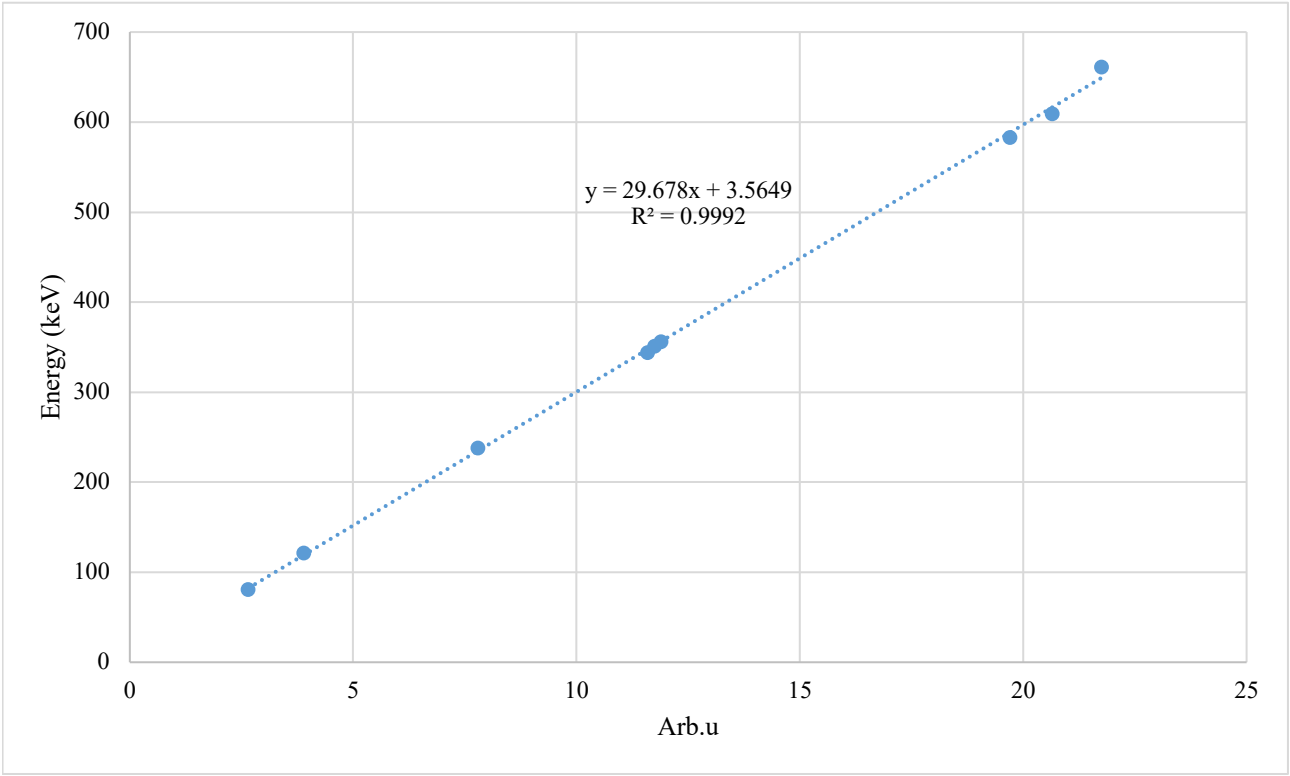

Fig. 44. Calibration curve of GS-JBUBG-85

3.6. Measurement of unknown rock

Unknown rock was found in Jáchymov, Czech Republic, where used to be a Uranium mine. From the looks (figure 45) it could be Uraninite.

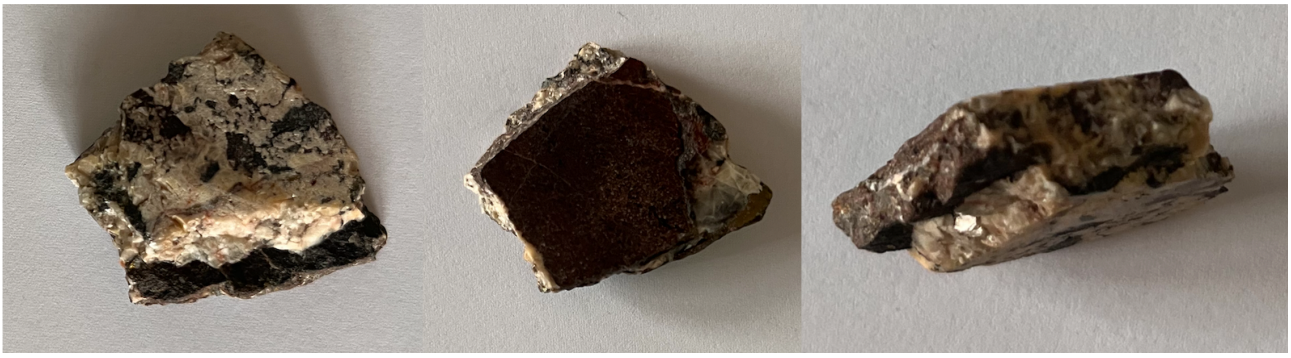

Fig. 45. Unknown rock from Jáchymov, Czech Republic

Background and unknown rock spectrums measured with GS-JBUBG-85 can be seen in figure 46. Unknown rock is about 25% more radioactive than background, with average CPM of 55, where background with constructed device is 44 counts per minute.

3.6.1. Manipulation of acquired unknown rock data

When measuring unknown radioactive material spectrum, and when the background radiation is subtracted, due to very low count number, each channel was averaged down with two its closest channels in both sides to get a smoother line. With such approach energy resolution has worsened, but it lets to see the peaks which were previously hard to notice.

3.6.2. Spectrum of unknown rock

If it is Uraninite, spectrum of such ore should have peaks at around 609.31 keV from ^{214}Bi and some smaller peaks like ^{226}Ra spectrum on energies of 186.10 keV(^{226}Ra) and 242.0 keV(^{214}Pb), 295.22 keV(^{214}Pb), and 351.31 keV(^{214}Pb), which all are the products of ^{235}U and ^{238}U decay [57,58].

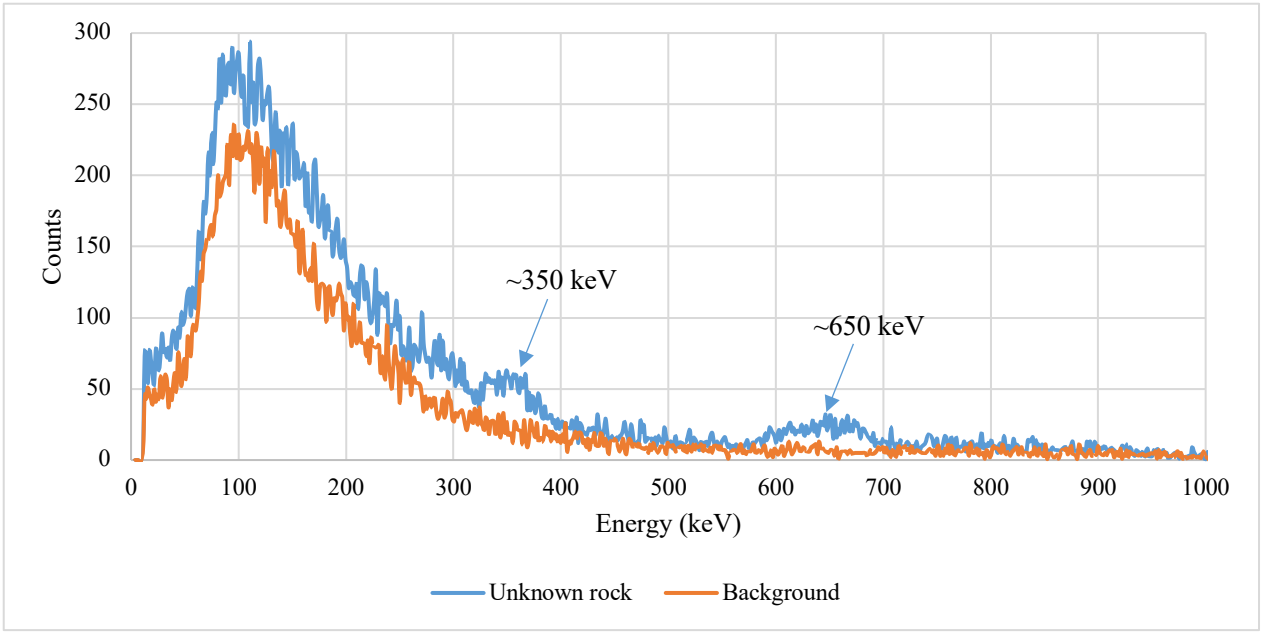

Fig. 46. Spectrum of unknown rock and background acquired with GS-JBUBG-85

From figure 46 it is obvious that some peaks at around 351.31 keV and 650 keV are present, yet it is quite hard to tell other peaks below 350 keV, so background counts were subtracted. Spectrum of unknown rock without background counts can be seen in figure 47.

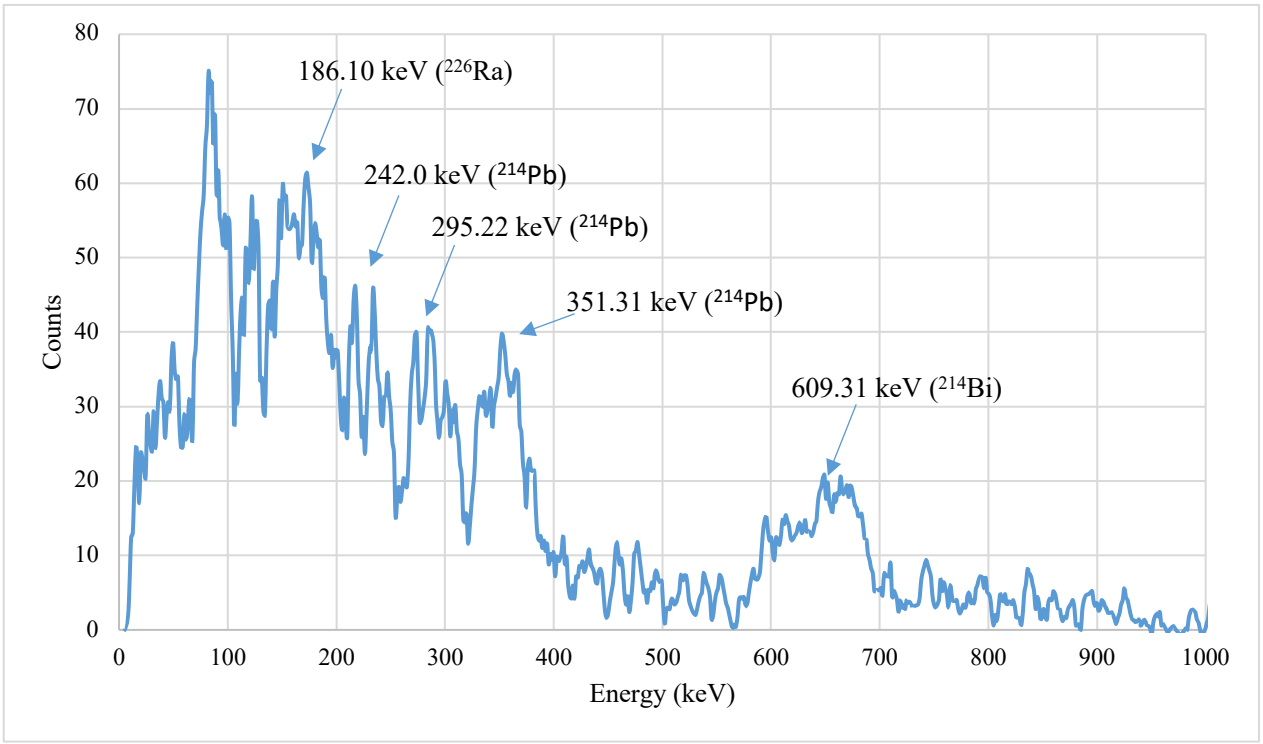

Fig. 47. Spectrum of unknown rock without background counts and averaged counts per channel

Now it is clearer and peaks of 186.10 keV, 242.0 keV, and 295.22 keV are visible in the spectrum. Since values were averaged, energy on abscissa axis does not exactly correspond to the peak energies, but from the shape of spectrum and the acquired data it is likely that hypothesis is accepted, and unknown material is Uraninite.

Conclusions

1. Literature and engineering analysis for developing open-source gamma spectrometer revealed that scintillation detector and photomultiplier tube synergy is the most suitable for "Do it Yourself" version of gamma spectrometer due to its ease of use and not requiring exotic equipment to run. Combination of both parts are able to transmit information about the energy of captured particle, yet it is important to understand what processes are happening inside and between these parts. Different characterization parameters are important and must be determined when developing and using scintillation counting based spectrometric solutions.
2. Constructed gamma spectrometry device uses 2.5 x 4 cm NaI(Tl) crystal, фэу – 85 photomultiplier. For signal processing and power supply "GS-USB-PRO" device with a multichannel analyzer was used. Whole system is designed to provide output signal either as pure audio level or digital data through USB. A special voltage divider and cabling was a big consideration in the design to limit the electronic noise influence during operation. Software defined parameters such as size of a channel, pulse shape method, minimum amplitude threshold values are critical when processing raw signal from detector.
3. Characterization of the developed device showed that фэу – 85 photomultiplier tube has a working voltage of 860V, where it showed most stable counts per minute number, as well as most fine energy resolution. System stability is obtained after 20 hours of on-time. Energy resolution of ^{137}Cs with the developed detector is 7.3%, which is 11.6% better than commercially manufactured device "IdentiFINDER" has. Also, signature energies of ^{137}Cs, ^{133}Ba, ^{228}Th, ^{152}Eu and ^{226}Ra are easily noticeable with constructed gamma spectrometer. As well as unknown radioactive material determination is also possible and Uraninite was successfully identified.

List of references

1. POŽĖLA, I, RADVILAVIČIUS Č. Fizika 2. Optika ir atomo fizika. Kaunas: KTU leidykla „Technologija“, 2011. ISBN 978-9955-25-910-7. page 177-178.
2. AMENOMORI, M., BAO, Y. W., BI, X. J., CHEN, D., CHEN, T. L., CHEN, W. Y., CUI, S. W. First Detection of Photons with Energy beyond 100 TeV from an Astrophysical Source. Physical Review Letters, vol. 123, no 5, 2019.
3. E.O. ECHEWEOZO, D.I. IGWESI, Investigation of gamma shielding and liquid permeability properties of kaolin for liquid radioactive waste management, Applied Radiation and Isotopes, vol 176, 2021.
4. HE JOHNS, JR CUNNINGHAM, Gamma and X-Ray Interactions in Matter, in Physics of Radiology, 4º ed. Illinois, USA, 1983, pp. 241–43.
5. KNOLL, G. F., Radiation Detection and Measurement 3rd ed, 1999
6. ADLIENĖ, D, ADLYS. G., Spinduliuotės detektoriai. Kaunas: KTU leidykla „Technologija“, 2011.
7. A. EL ABD, A method for determination mass absorption coefficient of gamma rays by Compton scattering, Applied Radiation and Isotopes, vol 94, 2014.
8. DR. JAMES E. PARKS. The Compton Effect – Compton Scattering and Gamma Ray Spectroscopy, Knoxville, Tennessee. 2015.
9. BORGHERESI, R., ADRIANI, O., ALBERGO, S., ANDREOTTI, M., CAPPELLO, G., CARDARELLI, P., VELTRI, M. A compton spectrometer to monitor the ELI-NP gamma beam energy. Nuclear Instruments and Methods in Physics Research Section A: Accelerators, Spectrometers, Detectors and Associated Equipment. 2018.
10. TARANJOT K, JEEWAN S., TEJBIR S., Review on scope of metallic alloys in gamma rays shield designing, Progress in Nuclear Energy, vol. 113, 2019.
11. REILLY, D, ENSSLIN, N, SMITH, H JR, AND KREINER, S. Passive nondestructive assay of nuclear materials. United States: N. p., 1991.
12. H. GEIGER AND W. MÜLLER, Electron counting tube for the measurement of the weakest radioactivities. 1928.
13. H. GEIGER AND W. MÜLLER,, W "Das Elektronenzählrohr". Physikalische Zeitschrift, 1929.
14. J.D. KURFESS, W.N. JOHNSON, R.A. KROEGER, B.F. PHLIPS, E.A. WULF, Development and applications of position-sensitive solid-state gamma ray detectors, Nuclear Instruments and Methods in Physics Research Section A: Accelerators, Spectrometers, Detectors and Associated Equipment, vol 505, Issues 1–2, 2003.
15. Used Field and Lab Radiological Instrumentation [online] [viewed 2022-01-12] Available from: https://nuclearstreet.com/buy-sell-nuclear-eqiupment/f/163/t/20675s.
16. P. MITRA, A. GUPTA, G. P. REDDY, S. SRIVASTAVA, M. TYAGI, M.K. SHARMA, S.C. GADKARI, P. CHAUDHURY, A. V. KUMAR, An environmental gamma spectrometry system with CsI(Tl) scintillator and FPGA based MCA for open field deployment, Applied Radiation and Isotopes, vol .172, 2021.
17. N. N. ASEMI, M. J. ALJAAFREH, S. PRASAD, S. ALDAWOOD, M. S. ALSALHI, Development of a gamma-ray scintillation detector based on blue-emitting oligomers and ZnO nanoparticles, Journal of King Saud University - Science, vol. 34, no. 4, 2022.

18. MOSZYNSKI, M. Energy resolution of scintillation detectors. Hard X-Ray and Gamma-Ray Detector Physics VII. 2005.
19. K.KOVLER , S.LEVINSON , N.LAVI , U.GHERMAN , B.DASHEVSKY , H.NASSAR , S.ANTROPOV, Scintillation vs. Semiconductor Spectrometers for Determination of NORM in Building Materials. NORM & Environmental Radioctivity. 2014.
20. D.T. MIHAILOVIC, S. AVDIC, A. MIHAILOVIC, Complexity measures and occurrence of the "breakpoint" in the neutron Radiation Physics and Chemistry. vol 184, July 2021.
21. LEO, W. R. Techniques for Nuclear and Particle Physics Experiments. 1994.
22. BIZARRI, G. Scintillation mechanisms of inorganic materials: From crystal characteristics to scintillation properties. Journal of Crystal Growth. 2010.
23. JAGTAP, S., CHOPADE, P., TADEPALLI, S., BHALERAO, A., & GOSAVI, S. A review on the progress of ZnSe as inorganic scintillator. Opto-Electronics Review. 2019.
24. J. R. LAMARSH, A. J. BARATTA, Introduction to Nuclear Engineering, 3d ed., Prentice-Hall, 2001.
25. PHOTOMULTIPLIER TUBES Basics and Applications THIRD EDITION (Edition 3a). HAMAMATSU PHOTONICS K. K. 2007.
26. LUBSANDORZHIEV, B. "On the history of photomultiplier tube invention". Nuclear Instruments and Methods in Physics Research Section A: Accelerators, Spectrometers, Detectors and Associated Equipment. 2006.
27. CURRAN, S. C. Counting tubes, theory and applications. Academic Press (New York). 1949.
28. U.S. Department of Energy, Instrumantation and Control. DOE Fundamentals Handbook, vol 2 of 2. June 1992.
29. MIRZOYAN, R., MÜLLER, D., HOSE, J., MENZEL, U., NAKAJIMA, D., TAKAHASHI, M., YAMAMOTO, T. Evaluation of novel PMTs of worldwide best parameters for the CTA project. Nuclear Instruments and Methods in Physics Research Section A: Accelerators, Spectrometers, Detectors and Associated Equipment. 2017.
30. FAZEKAS, B., RÉVAY, Z., ÖSTÖR, J., BELGYA, T., MOLNÁR, G., & SIMONITS, A. A new method for determination of gamma-ray spectrometer non-linearity. Nuclear Instruments and Methods in Physics Research Section A: Accelerators, Spectrometers, Detectors and Associated Equipment. 1999.
31. DMITRENKO, V. V., ULIN, S. E., GRACHEV, V. M., VLASIK, K. F., UTESHEV, Z. M., CHERNYSHEVA, I. V., DUKHVALOV, A. G. (n.d.). Perspectives of High Pressure Xenon Gamma-Ray Spectrometers to Detect and Identify Radioactive and Fissile Materials. Prevention, Detection and Response to Nuclear and Radiological Threats. 2008.
32. ZENG, G., TAN, C., LI, Q., GE, L., LIU, X., & LUO, Q. Reset charge sensitive amplifier for NaI(Tl) gamma-ray spectrometer. Applied Radiation and Isotopes. 2015.
33. R.L. BELL: "Negative Electron Affinity Devices", Clarendon Press. 1973.
34. MCGRAW-HILL "Handbook of Optics". 1978.
35. RICHARD D. DESLATTES, Journal of Research of the National Institute of Standards and Technology, High Resolution γ-Ray Spectroscopy: the First 85 Years. 2000.
36. Power supply [online] [viewed 2022-05-05] Available from: https://www.distrelec.lt/Web/WebShopImages/landscape_large/4-/01/1082314-01.jpg
37. VEIT B. M., Active Voltage Dividers for Photomultipliers. March 2019.

38. Photomultiplier tube basics [online] [viewed 2022-05-11] Available from: https://psec.uchicago.edu/library/photomultipliers/Photonis_PMT_basics.pdf
39. DAMBACHER, M., ZWERGER, A., FAULER, A., DISCH, C., STÖHLKER, U., & FIEDERLE, M. Development of the gamma-ray analysis digital filter multi-channel analyzer (GMCA). Nuclear Instruments and Methods in Physics Research Section A: Accelerators, Spectrometers, Detectors and Associated Equipment. 2011.
40. LIMA, H. P., GUEDES, G. P., BARBOSA, A. F., & SEIXAS, J. M. A Fast Multichannel-Analyzer for Radiation Detection Applications. IEEE Transactions on Instrumentation and Measurement. 2004.
41. Gamma Spectroscopy Software [online] [viewed 2022-05-11] Available from: https://www.gammaspectacular.com/blue/pra-spectrometry-software
42. JEFFREY P, VESILIND P A, RUTH W. Environmental Pollution and Control (Fourth Edition) 1998.
43. Ankstyvojo radiacinio pavojaus perspėjimo sistema (RADIS) [online] [viewed 2022-05-12] Available from: https://www.rsc.lt/index.php/pageid/1196
44. Ankstyvojo radiacinio pavojaus perspėjimo sistema (RADIS) [online] [viewed 2022-05-12] Available from: https://www.labochema.lt/radis/#
45. SARA – SPECTROSCOPIC GAMMA DETECTOR [online] [viewed 2022-01-12] Available from: https://envinet.com/images/produkte/sara/data_sheet_sara_detector.pdf
46. The nationwide RadNet system [online] [viewed 2022-05-12] Available from: https://www.epa.gov/radnet/learn-about-radnet
47. IdentiFINDER [online] [viewed 2022-05-12] Available from: https://www.flir.com/products/identifinder-r400/#
48. ПРИБОР ГЕОЛОГОРАЗВЕДОЧНЫЙ СЦИНТИЛЛЯЦИОННЫЙ СРП-88Н Сборочные чертежи, схемы и перечни элементов. Алъбом № 1 ЖШ 1.289.386 ОП
49. FEU-85 [online] [viewed 2022-05-21] Available from: https://eandc.ru/pdf/opto/feu-85.pdf
50. Recommended Nuclear Decay Data Ba-133 [online] [viewed 2022-05-22] Available from: http://www.nucleide.org/DDEP_WG/Nuclides/Ba-133_tables.pdf
51. Recommended Nuclear Decay Data Ba-133 [online] [viewed 2022-05-22] Available from: https://www.ezag.com/fileadmin/ezag/user-uploads/isotopes/isotopes/Isotrak/isotrak-pdf/Decay_Schema_Data/Ba-133.pdf
52. Recommended Nuclear Decay Data Th-232 [online] [viewed 2022-05-22] Available from: https://www.ld-didactic.de/software/524221en/Content/Appendix/Th232.htm
53. Recommended Nuclear Decay Data Th-232 [online] [viewed 2022-05-22] Available from: http://www.lnhb.fr/nuclides/Th-228_tables.pdf
54. Recommended Nuclear Decay Data Th-232 [online] [viewed 2022-05-22] Available from: https://www.radiochemistry.org/periodictable/gamma_spectra/pdf/th228.pdf
55. Recommended Nuclear Decay Data Eu-152 [online] [viewed 2022-05-22] Available from: https://www.ezag.com/fileadmin/ezag/user-uploads/isotopes/isotopes/Isotrak/isotrak-pdf/Decay_Schema_Data/Eu-152.pdf
56. Recommended Nuclear Decay Data Ra-226 [online] [viewed 2022-05-22] Available from: https://www.ezag.com/fileadmin/ezag/user-uploads/isotopes/isotopes/Isotrak/isotrak-pdf/Decay_Schema_Data/Ra-226.pdf
57. Recommended Nuclear Decay Data U-238 [online] [viewed 2022-05-22] Available from: https://www.ezag.com/fileadmin/ezag/user-uploads/isotopes/isotopes/Isotrak/isotrak-pdf/Decay_Schema_Data/U-238.pdf

58. Recommended Nuclear Decay Data U-235 [online] [viewed 2022-05-22] Available from: http://www.nucleide.org/DDEP_WG/Nuclides/U-235_tables.pdf

Appendices

Appendix 1. Spectrums of known sources acquired with GS-JBUBG-85

In these figures spectrums of known sources acquired with calibrated GS-JBUBG-85 are shown.

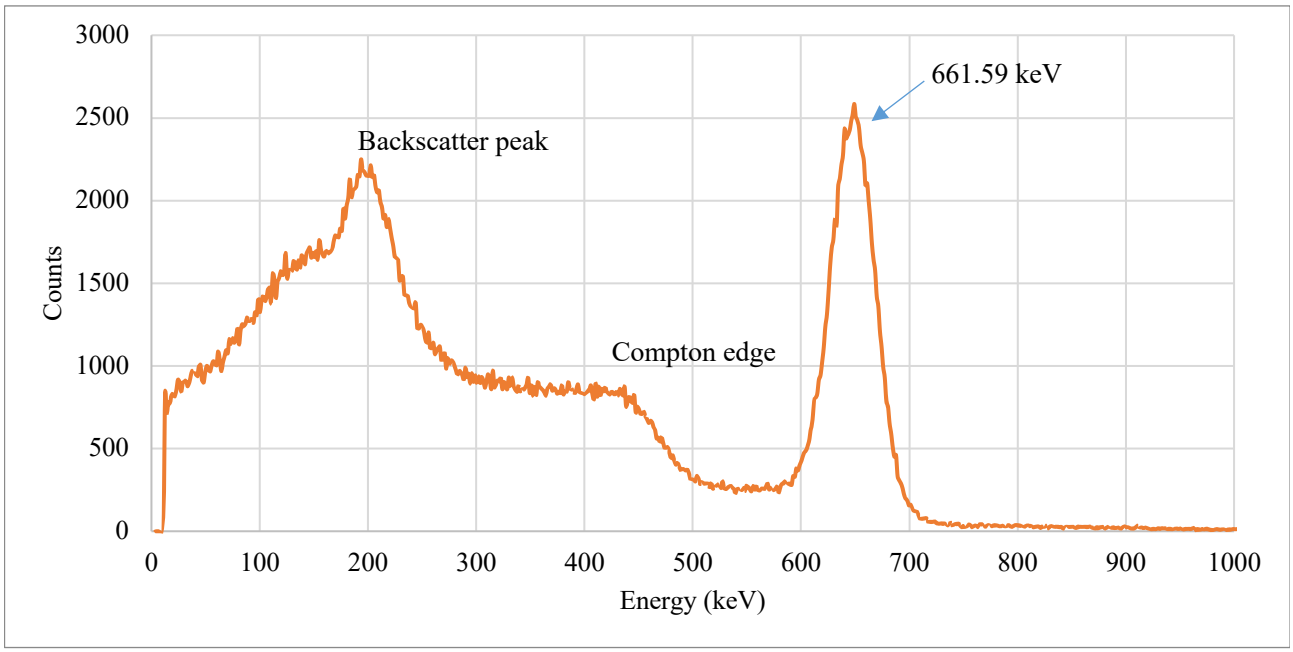

Fig. 48. Spectrum of ^{137}Cs

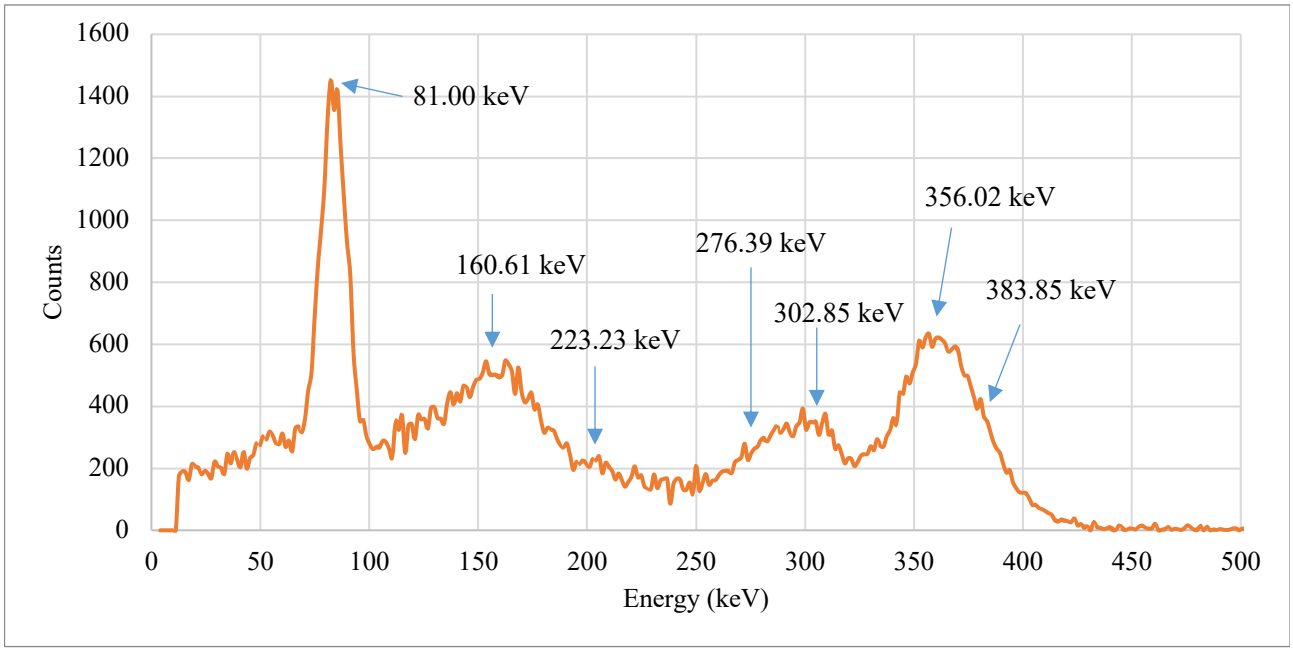

Fig. 49. Spectrum of ^{133}Ba

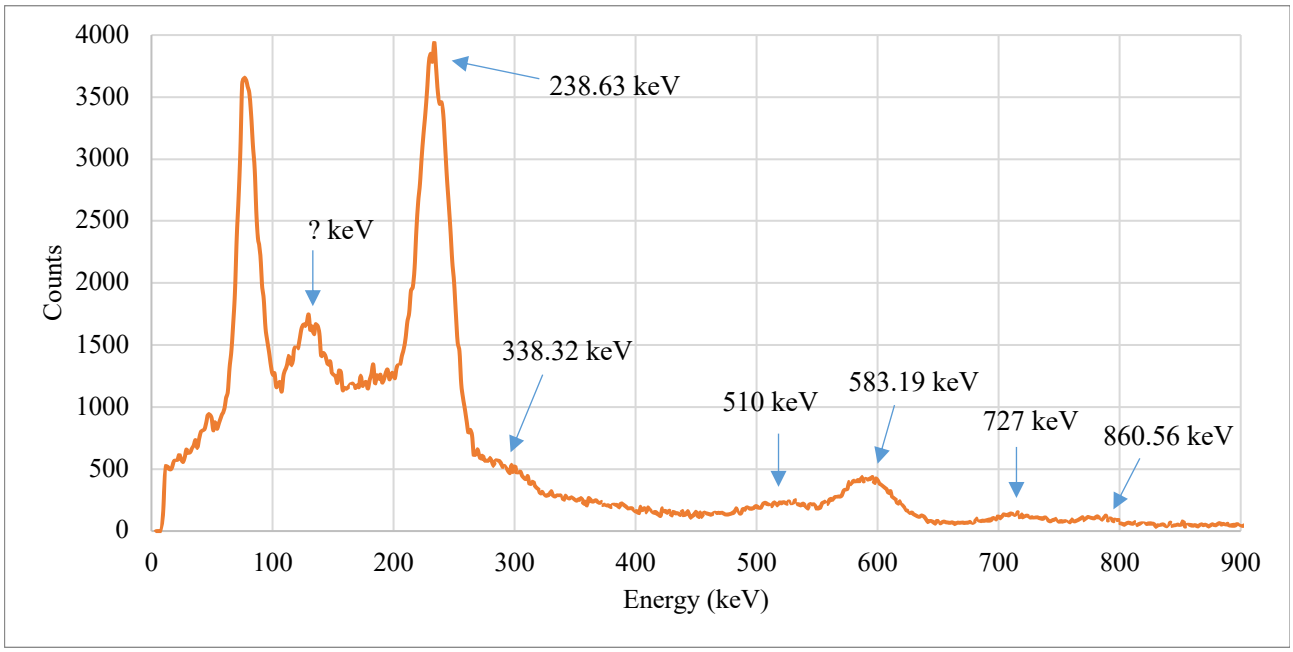

Fig. 50. Spectrum of ^{228}Th

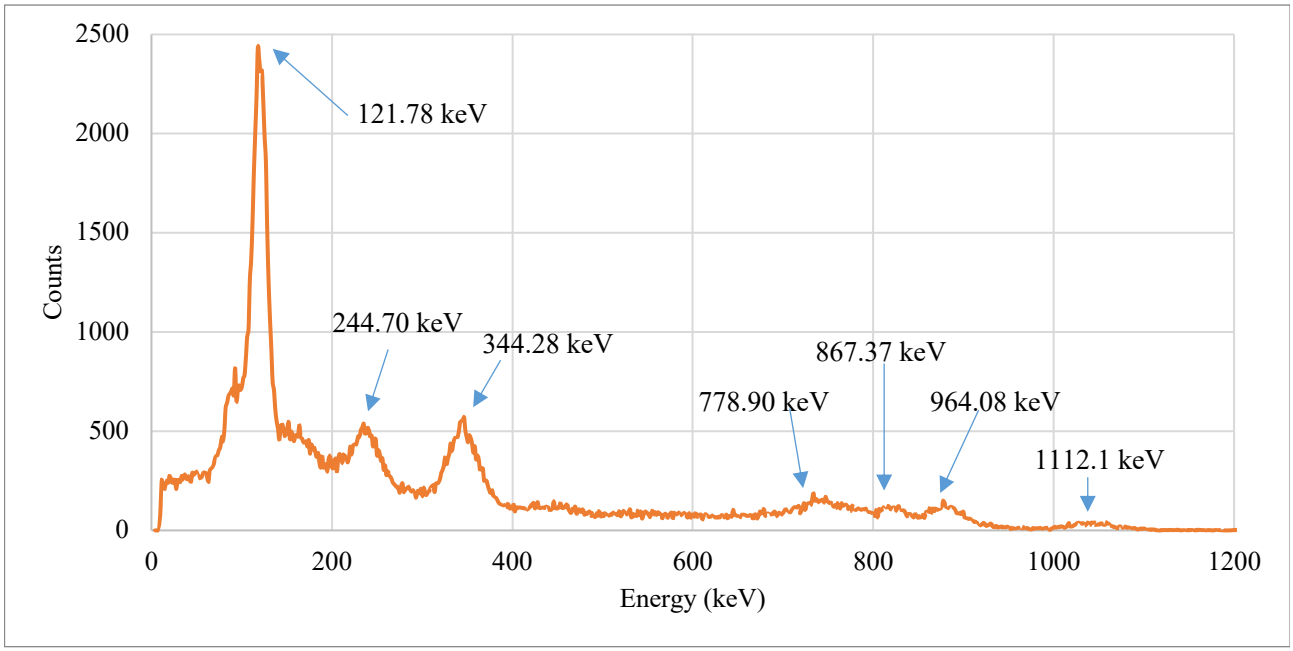

Fig. 51. Spectrum of ^{152}Eu

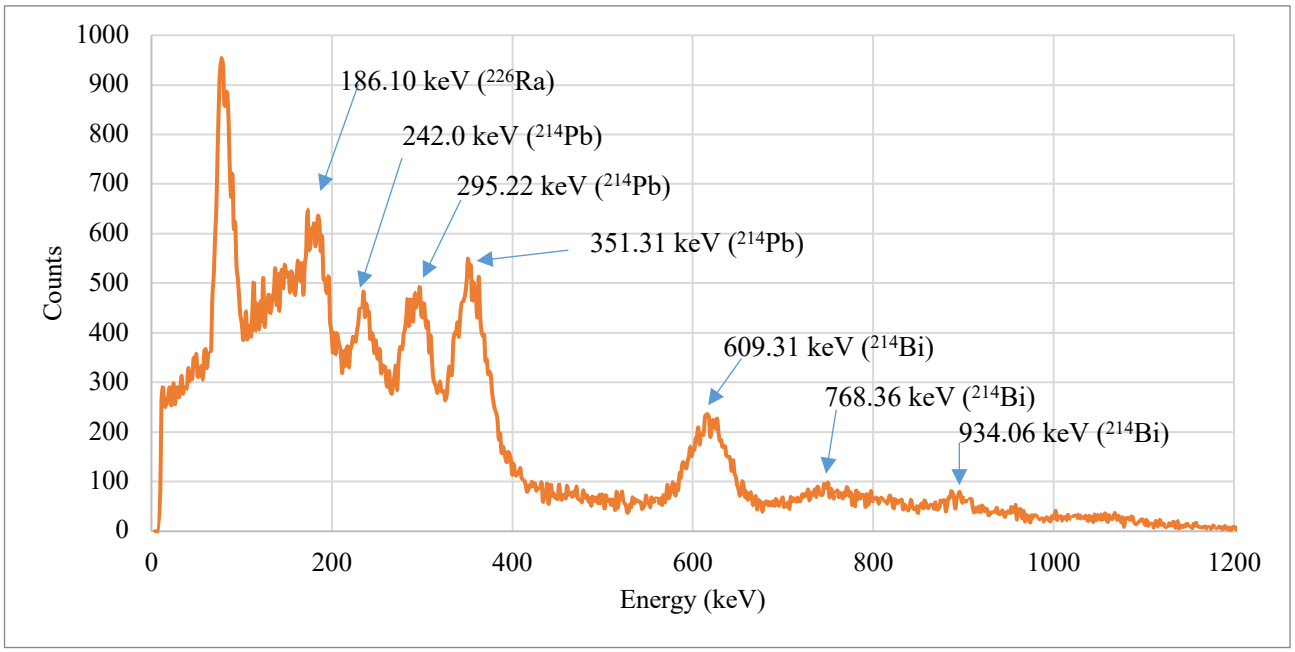

Fig. 52. Spectrum of ^{226}Ra

Appendix 2. Spectrum of unknown rock acquired with GS-JBUBG-85

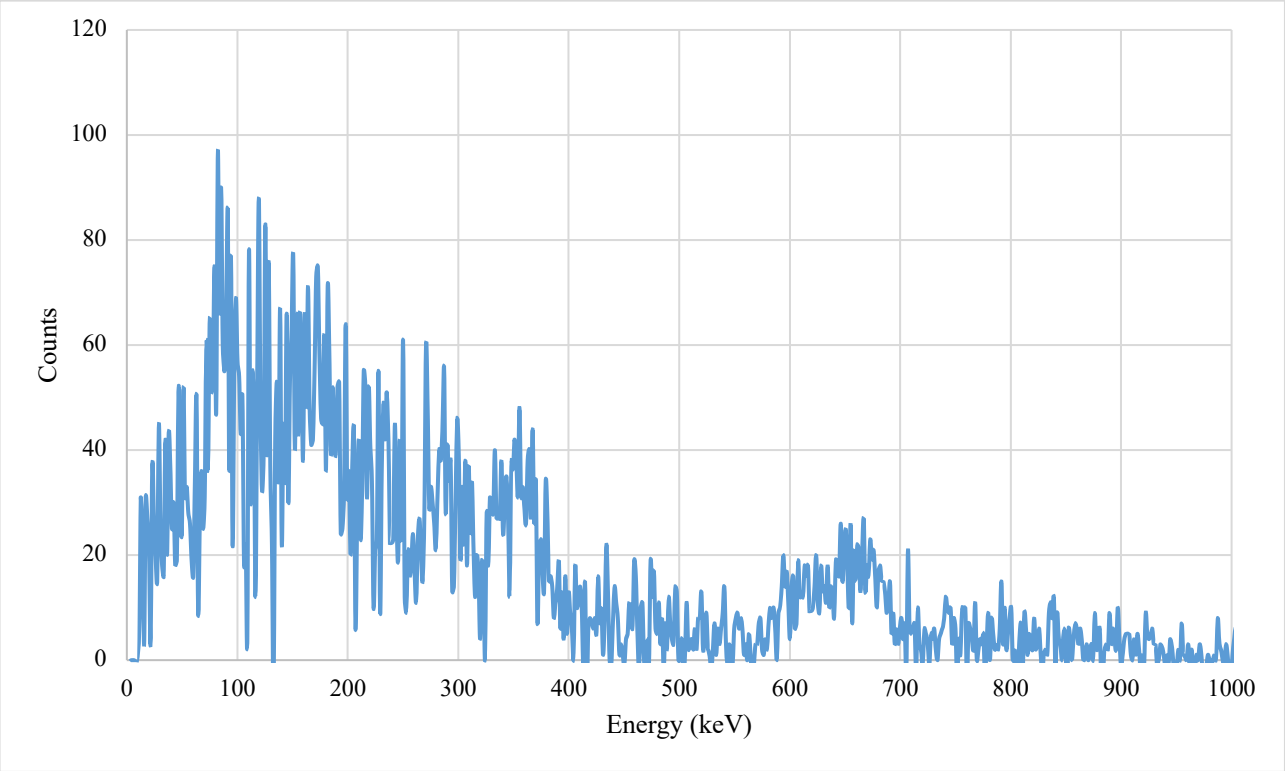

Fig. 53. Raw spectrum of unknown rock with subtracted background counts